A NONCOFORMING VIRTUAL ELEMENT APPROXIMATION FOR THE OSEEN EIGENVALUE PROBLEM*

DIBYENDU ADAK[†], FELIPE LEPE[‡], AND GONZALO RIVERA[§]

Abstract. In this paper we analyze a nonconforming virtual element method to approximate the eigenfunctions and eigenvalues of the two dimensional Oseen eigenvalue problem. The spaces under consideration leads to a divergence-free method which is capable to capture properly the divergence at discrete level and the eigenvalues and eigenfunctions. Under the compact theory for operators we prove convergence and error estimates for the method. By employing the theory of compact operators we recovered the double order of convergence of the spectrum. Finally, we present numerical tests to assess the performance of the proposed numerical scheme.

Key words. Oseen equations, eigenvalue problems, virtual element method

AMS subject classifications. 35Q35, 65N15, 65N25, 65N30, 65N50

1. Introduction.

The numerical approximation of partial differential equations, and the analysis of schemes to approximate the solution of classical models in the pure and applied sciences, is a well-established topic. In particular, the numerical analysis for eigenvalue problems arising from fluid mechanics has paid the attention for researchers from several years, and the literature attending this topic is abundant. We mention [1, 7, 17, 16, 25, 26, 30, 28, 19] as some references on this topic.

The common aspect of the above references of the mentioned eigenvalue problems are related to the Stokes equations, where the particularity is that the resulting eigenvalue problem results to be selfadjoint and hence, symmetric. This is a desirable feature since we deal with real eigenvalues and eigenfunctions. Now the task is different, since our research program is devoted to the study of non-selfadjoint eigenvalue problems in fluid mechanics, in particular the Oseen eigenvalue problem and hence, the well developed theory for the Stokes eigenvalue problem must be extended.

The Oseen equations are a linearization of the Navier-Stokes equations and a complete analysis of the source problem for the Oseen system is available in [20]. Here is presented the motivation on the need to study the Oseen system, since to solve the time dependent Navier-Stokes equations, it is necessary to solve a linear system in each step of time which, precisely is an Oseen type of system. With this motivation at hand, our task is to analyze numerically the Oseen eigenvalue problem with the aid of a virtual element method (VEM).

The VEM possesses many remarkable features that make it an attractive numerical strategy for engineering and mathematical communities in order to solve different model problems. In a general view, the most important features of the VEM are a solid mathematical background, the capability of combine elements irrespective of

*Submitted to the editors DATE.

Funding: DA and FL were partially supported by DIUBB through project 2120173 GI/C Universidad del Bío-Bío. FL was partially supported by ANID-Chile through FONDECYT project 11200529 (Chile). GR was supported by Universidad de Los Lagos Regular R02/21 and ANID-Chile through FONDECYT project 1231619 (Chile).

[†]GIMNAP-Departamento de Matemática, Universidad del Bío-Bío, Casilla 5-C, Concepción, Chile. dadak@ubiobio.cl.

[‡]GIMNAP-Departamento de Matemática, Universidad del Bío-Bío, Casilla 5-C, Concepción, Chile. flepe@ubiobio.cl.

[§]Departamento de Ciencias Exactas, Universidad de Los Lagos, Osorno, Chile. gonzalo.rivera@ulagos.cl

geometric shapes, including nonconvex and oddly shaped elements, arbitrary orders of accuracy and regularity, the easy extension to higher dimensions, among others. A recent state of art of the VEM and its applications is available in [5].

In the present work we are interested in the application of a nonconforming virtual element method (NCVEM) to solve the nonsymmetric Oseen eigenvalue problem. The NCVEM, introduced in [9], has been applied in different elliptic problems such as [6, 8, 14, 29, 34, 35] and in particular for eigenvalue problems we mention [3, 2, 15] as interesting references with excellent results for the discretization of the corresponding spectrums.

For the Oseen eigenvalue problem, we need an inf-sup stable NCVEM for the Stokes source problem which is available in [35]. This family of NCVEM has also the capability of holding the incompressibility condition at discrete level, which is a desirable feature that also is already available for the conforming VEM [13].

Recently in [27] and for the best of the author's knowledge, appears a finite element approximation for the Oseen eigenvalue problem as a novel effort to solve numerically this problem. Since the problem is non-symmetric, the ad-hoc strategy for the analysis is the introduction of the dual eigenvalue problem in order to obtain error estimates for the method, following the well known theory of [10]. Clearly for the NCVEM approach the strategy is similar but not exactly the same, since the lack of conformity carries extra terms due the variational crime that a non conforming method naturally involves and must be correctly controlled. Clearly this must be done for both, the primal and dual eigenvalue problems.

The formulation under consideration on this paper is the classic velocity-pressure formulation which has the advantage of using the simplest virtual spaces for the approximation. On the other hand, despite to the fact that the method is non-conforming, the solution operator that we define for our work is defined form $\mathbf{L}^2$ to $\mathbf{L}^2$ and allows us to utilize the classic theory for compact operators to carry out the convergence and error analysis of the method similarly as in [15]. Moreover, in our contribution we derive an $\mathbf{L}^2$ error estimate for the velocity via a duality argument, delivering an improvement on the error estimates for this variable.

Theoretically, we are capable to prove that the proposed NCVEM is spurious free according to the theory of [21], which is a consequence of the convergence in norm for compact operators. However, in the numerical section, we report that similarly as in the continuous VEM framework (see [24, 25] for instance), the stabilization terms of the NCVEM may also introduce spurious eigenvalues and must be avoided.

The paper is organized as follows: In Section 2 we introduce the Oseen eigenvalue problem and associated weak formulation. We present the functional framework in which the papers is based, namely Hilbert spaces, norms, the variational formulation, regularity of the source and spectral problems, and the solution operator in the same section. All this must be defined for the primal and dual eigenvalue problems. In Section 3, we have recollected the divergence-free nonconforming VEM space and discrete formulation of the weak form. The discrete solution operator is also defined in the same section. The a priori error estimates for the source problem in L^2, and broken H^1 norms are defined in the Section 4. Eventually, in Section 5, we have proved the double order of convergence of the spectrum. In Section 6, we have assessed some numerical experiments as an evidence of the theoretical estimates.

1.1. Notation and Preliminaries. Given any Hilbert space X, we define $\mathbf{X} := \mathrm{X}^2$, the space of vectors with entries in X. For any scalar field φ and vector field $\boldsymbol{u}$, we introduce the following differential operators: the **curl** of φ, defined as $\mathbf{curl}\varphi =$

$(\partial_2\varphi, -\partial_1\varphi)^{\mathtt{t}}$ where $\mathtt{t}$ represents the transpose operator; the gradient of $\boldsymbol{u}$, defined as the matrix $(\nabla\boldsymbol{u}) = (\partial_j u_i)_{i,j=1,2}$; the rotor of $\boldsymbol{u}$, defined as $\operatorname{rot}\boldsymbol{u} = \partial_2 u_1 - \partial_1 u_2$; the divergence of $\boldsymbol{u}$, defined as $\operatorname{div}\boldsymbol{u} = \partial_1 u_1 + \partial_2 u_2$. Given $\mathbf{A} := (A_{ij}), \mathbf{A} := (A_{ij}) \in \mathbb{C}^{2\times 2}$, we define $\mathbf{A} : \mathbf{B} := \sum_{i,j=1}^{2} A_{ij}\overline{B_{ij}}$ as the tensorial product between $\mathbf{A}$ and $\mathbf{B}$. The entry $\overline{B_{ij}}$ represent the complex conjugate of B_{ij}. Similarly, given two vectors $\mathbf{s} = (s_i), \mathbf{r} = (r_i) \in \mathbb{C}^2$, we define the products

$$\mathbf{s}\cdot\mathbf{r} := \sum_{i=1}^{2} s_i\overline{r_i} \qquad \mathbf{s}\otimes\mathbf{r} := \mathbf{s}\overline{\mathbf{r}}^{\mathtt{t}} = (s_i\overline{r_j})_{1\leq i,j\leq 2},$$

as the dot and dyadic product in $\mathbb{C}$. Further, we recollect the definition $\operatorname{div}(\mathbf{A}) := (\sum_{j=1}^{2}\partial_j A_{ij})_{i=1,2}$.

2. The variational formulation. Let us describe the model of our study. From now and on, $\Omega \subset \mathbb{R}^2$ represents an open bounded polygonal/polyhedral domain with Lipschitz boundary $\partial\Omega$. The equations of the Oseen eigenvalue problem are given as follows:

$$(2.1)\qquad \left\{\begin{array}{rcll} -\nu\Delta\boldsymbol{u} + (\boldsymbol{\beta}\cdot\nabla)\boldsymbol{u} + \nabla p & = & \lambda\boldsymbol{u} & \text{in}\,\Omega,\\ \operatorname{div}\boldsymbol{u} & = & 0 & \text{in}\,\Omega,\\ \displaystyle\int_\Omega p & = & 0, & \text{in}\,\Omega,\\ \boldsymbol{u} & = & \mathbf{0}, & \text{on}\,\partial\Omega, \end{array}\right.$$

where $\boldsymbol{u}$ is the displacement, p is the pressure and $\boldsymbol{\beta}$ is a given vector field, representing a *steady flow velocity* and $\nu > 0$ is the kinematic viscosity.

Through our paper, we assume the existence of two positive numbers ν^+ and ν^- such that $\nu^- < \nu < \nu^+$. On the other hand, we assume that $\boldsymbol{\beta} \in \mathbf{L}^\infty(\Omega, \mathbb{C})$. For the kinematic viscosity and the steady flow velocity we assume the following standard assumptions (see [20]):

- $\|\boldsymbol{\beta}\|_{\infty,\Omega} \sim 1$ if $\nu \leq \|\boldsymbol{\beta}\|_{\infty,\Omega}$,
- $\nu \sim 1$ if $\|\boldsymbol{\beta}\|_{\infty,\Omega} < \nu$.

Regarding the convective term, let us assume that there exists a constant $\varepsilon_1 > 0$ such that $\boldsymbol{\beta} \in \mathbf{L}^{2+\varepsilon_1}(\Omega, \mathbb{C})$ that leads to the skew-symmetry of the convective term (see [20, Remark 5.6]) which claims that for all $\boldsymbol{v} \in \mathbf{H}_0^1(\Omega, \mathbb{C})$, there holds

$$(2.2)\qquad \int_\Omega (\boldsymbol{\beta}\cdot\nabla)\boldsymbol{v}\cdot\boldsymbol{v} = 0 \quad \forall \boldsymbol{v} \in \mathbf{H}_0^1(\Omega, \mathbb{C}).$$

Now we introduce the functional spaces and norms for our analysis. Let us define the spaces $\mathcal{X} := \mathbf{H}_0^1(\Omega, \mathbb{C}) \times \mathrm{L}_0^2(\Omega, \mathbb{C})$ together with the space $\mathcal{Y} := \mathbf{H}_0^1(\Omega, \mathbb{C}) \times \mathbf{H}_0^1(\Omega, \mathbb{C})$. For the space $\mathcal{X}$ we define the norm $\|\cdot\|_{\mathcal{X}}^2 := \|\cdot\|_{1,\Omega}^2 + \|\cdot\|_{0,\Omega}^2$ whereas for $\mathcal{Y}$ the norm will be $\|(\boldsymbol{v}, \boldsymbol{w})\|_{\mathcal{Y}}^2 = \|\boldsymbol{v}\|_{1,\Omega}^2 + \|\boldsymbol{w}\|_{1,\Omega}^2$, for all $(\boldsymbol{v}, \boldsymbol{w}) \in \mathcal{Y}$.

Let us introduce the following sesquilinear forms $a : \mathcal{Y} \to \mathbb{C}$ and $b : \mathcal{X} \to \mathbb{C}$ defined by

$$a(\boldsymbol{w}, \boldsymbol{v}) := a_{\mathrm{sym}}(\boldsymbol{w}, \boldsymbol{v}) + a_{\mathrm{skew}}(\boldsymbol{w}, \boldsymbol{v}) \quad \text{and} \quad b(\boldsymbol{v}, q) := -\int_\Omega q \operatorname{div}\boldsymbol{v},$$

where $a_{\mathrm{sym}}, a_{\mathrm{skew}} : \mathcal{Y} \to \mathbb{C}$ are two sesquilinear forms defined by

$$a_{\mathrm{sym}}(\boldsymbol{w}, \boldsymbol{v}) := \int_\Omega \nu\nabla\boldsymbol{w} : \nabla\boldsymbol{v} \quad \text{and} \quad a_{\mathrm{skew}}(\boldsymbol{w}, \boldsymbol{v}) := \frac{1}{2}\Big(a^{\boldsymbol{\beta}}(\boldsymbol{w}, \boldsymbol{v}) - a^{\boldsymbol{\beta}}(\boldsymbol{v}, \boldsymbol{w})\Big),$$

where, $a^{\boldsymbol{\beta}}(\boldsymbol{w},\boldsymbol{v}) := \int_\Omega (\boldsymbol{\beta}\cdot\nabla)\boldsymbol{w}\cdot\boldsymbol{v}$. On the other hand we define the following sesquilinear form $c(\boldsymbol{w},\boldsymbol{v}) := (\boldsymbol{w},\boldsymbol{v})_{0,\Omega}$ as the standard inner product in $\mathbf{L}^2(\Omega,\mathbb{C})$. With these sesquilinear forms at hand, we write the following weak formulation for (2.1): Find $\lambda\in\mathbb{C}$ and $(\mathbf{0},0)\neq(\boldsymbol{u},p)\in\mathcal{X}$ such that

$$\text{(2.3)}\qquad \left\{\begin{array}{rcll} a(\boldsymbol{u},\boldsymbol{v})+b(\boldsymbol{v},p) &=& \lambda c(\boldsymbol{u},\boldsymbol{v}) & \forall \boldsymbol{v}\in\mathbf{H}_0^1(\Omega,\mathbb{C}),\\ b(\boldsymbol{u},q) &=& 0 & \forall q\in \mathrm{L}_0^2(\Omega,\mathbb{C}),\end{array}\right.$$

where

$$\mathrm{L}_0^2(\Omega,\mathbb{C}) := \left\{ q\in\mathrm{L}^2(\Omega,\mathbb{C}) \,:\, \int_\Omega q = 0\right\}.$$

Observe that the resulting eigenvalue problem is non-symmetric due the presence of the sesquilinear form $a^{\boldsymbol{\beta}}(\cdot,\cdot)$. Let us define the kernel $\mathcal{K}$ of $b(\cdot,\cdot)$ as follows

$$\mathcal{K} := \{\boldsymbol{v}\in\mathbf{H}_0^1(\Omega,\mathbb{C}) \,:\, b(\boldsymbol{v},q)=0 \;\;\forall q\in\mathrm{L}_0^2(\Omega,\mathbb{C})\}.$$

With this space available, it is straightforward to verify using (2.2) that $a(\cdot,\cdot)$ is $\mathcal{K}$-coercive. Moreover, the bilinear form $b(\cdot,\cdot)$ satisfies the following inf-sup condition

$$\text{(2.4)}\qquad \sup_{\boldsymbol{\tau}\in\mathbf{H}_0^1(\Omega,\mathbb{C})} \frac{b(\boldsymbol{\tau},q)}{\|\boldsymbol{\tau}\|_{1,\Omega}} \geq \beta\|q\|_{0,\Omega} \quad \forall q\in\mathrm{L}_0^2(\Omega,\mathbb{C}).$$

Let us introduce the solution operator, which we denote by $\boldsymbol{T}$ and is defined as follows

$$\text{(2.5)}\qquad \boldsymbol{T}:\mathbf{L}^2(\Omega,\mathbb{C})\to\mathbf{L}^2(\Omega,\mathbb{C}),\qquad \boldsymbol{f}\mapsto\boldsymbol{T}\boldsymbol{f}:=\widehat{\boldsymbol{u}},$$

where the pair $(\widehat{\boldsymbol{u}},\widehat{p})\in\mathcal{X}$ is the solution of the following well-posed source problem

$$\text{(2.6)}\qquad \left\{\begin{array}{rcll} a(\widehat{\boldsymbol{u}},\boldsymbol{v})+b(\boldsymbol{v},\widehat{p}) &=& c(\boldsymbol{f},\boldsymbol{v}) & \forall \boldsymbol{v}\in\mathbf{H}_0^1(\Omega,\mathbb{C}),\\ b(\widehat{\boldsymbol{u}},q) &=& 0 & \forall q\in \mathrm{L}_0^2(\Omega,\mathbb{C}),\end{array}\right.$$

implying that $\boldsymbol{T}$ is well defined due to the Babuška-Brezzi theory. Moreover, from [20, Lemma 5.8] we have the following estimates for the velocity and pressure, respectively

$$\|\nabla\widehat{\boldsymbol{u}}\|_{0,\Omega} \leq \frac{C_{pf}}{\nu}\|\boldsymbol{f}\|_{0,\Omega},$$

$$\|\widehat{p}\|_{0,\Omega}^2 \leq \frac{1}{\beta}\left(\|\boldsymbol{f}\|_{0,\Omega} + \nu^{1/2}\|\nabla\widehat{\boldsymbol{u}}\|_{0,\Omega}\left(\nu^{1/2} + C_{pf}\frac{\|\boldsymbol{\beta}\|_{0,\infty}}{\nu^{1/2}}\right)\right),$$

where $C_{pf}>0$ represents the constant of the Poincaré-Friedrichs inequality and $\beta>0$ is the inf-sup constant given un (2.4).

It is easy to check that $(\lambda,(\boldsymbol{u},p))\in\mathbb{C}\times\mathcal{X}$ solves (2.3) if and only if $(\kappa,\boldsymbol{u})$ is an eigenpair of $\boldsymbol{T}$, *i.e.*, $\boldsymbol{T}\boldsymbol{u}=\kappa\boldsymbol{u}$ with $\kappa:=1/\lambda$ and $\lambda\neq 0$.

A key point for the analysis is the additional regularity of the solution. To obtain this, the assumptions on $\boldsymbol{\beta}$ are important,. To make matters precise, if the convective term is well defined, it is possible to resort to the classic Stokes regularity results available on the literature (see [32] for instance). Hence, the following additional regularity result for the solutions of the Oseen system holds.

THEOREM 2.1. *There exists $s>0$ that for all $\boldsymbol{f}\in\mathbf{L}^2(\Omega,\mathbb{C})$, the solution $(\widehat{\boldsymbol{u}},\widehat{p})\in\mathcal{X}$ of problem (2.6), satisfies for the velocity $\widehat{\boldsymbol{u}}\in\mathbf{H}^{1+s}(\Omega,\mathbb{C})$, for the pressure $\widehat{p}\in\mathrm{H}^s(\Omega,\mathbb{C})$, and*

$$\|\widehat{\boldsymbol{u}}\|_{1+s,\Omega} + \|\widehat{p}\|_{s,\Omega} \leq C\|\boldsymbol{f}\|_{0,\Omega},.$$

where $C := \dfrac{C_{pf}}{\beta}\max\left\{1, \dfrac{C_{pf}\|\boldsymbol{\beta}\|_{\infty,\Omega}}{\nu}\right\}$ *and* $\beta > 0$ *is the constant associated to the inf-sup condition* (2.4). *Further, if* $(\boldsymbol{u}, p)$ *is an eigenfunction satisfying* (2.3)*, then there exists* $r > 0$*, not necessarily equal to* s*, such that* $(\boldsymbol{u}, p) \in \mathcal{X} \cap (\mathbf{H}^{1+r}(\Omega,\mathbb{C}) \times \mathrm{H}^{r}(\Omega,\mathbb{C}))$ *and the following bound holds*

$$\|\widehat{\boldsymbol{u}}\|_{1+r,\Omega} + \|\widehat{p}\|_{r,\Omega} \leq C\|\widehat{\boldsymbol{u}}\|_{0,\Omega}.$$

Observe that the following compact inclusion $\mathbf{H}^{1+s}(\Omega,\mathbb{C}) \hookrightarrow \mathbf{L}^2(\Omega,\mathbb{C})$, implying directly the compactness of $\boldsymbol{T}$. Finally, we have the following spectral characterization for $\boldsymbol{T}$.

LEMMA 2.2. *(Spectral Characterization of* $\boldsymbol{T}$*). The spectrum of* $\boldsymbol{T}$ *is such that* $\mathrm{sp}(\boldsymbol{T}) = \{0\} \cup \{\kappa_k\}_{k\in N}$ *where* $\{\kappa_k\}_{k\in\mathbf{N}}$ *is a sequence of complex eigenvalues that converge to zero, according to their respective multiplicities.*

We conclude this section by redefining the spectral problem (2.3) in order to simplify the notations for the forthcoming analysis. With this in mind, let us introduce the sesquilinear form $A : \mathcal{X} \times \mathcal{X} \to \mathbb{C}$ defined by

$$A((\boldsymbol{u}, p); (\boldsymbol{v}, q)) := a(\boldsymbol{u}, \boldsymbol{v}) + b(\boldsymbol{v}, p) - b(\boldsymbol{u}, q), \quad \forall (\boldsymbol{v}, q) \in \mathcal{X},$$

which allows us to rewrite problem (2.3) as follows: Find $\lambda \in \mathbb{C}$ and $(\mathbf{0}, 0) \neq (\boldsymbol{u}, p) \in \mathcal{X}$ such that

$$A((\boldsymbol{u}, p), (\boldsymbol{v}, q)) = \lambda c(\boldsymbol{u}, \boldsymbol{v}) \quad \forall (\boldsymbol{v}, q) \in \mathcal{X}. \tag{2.7}$$

Since the problem is non-selfadjoint, it is necessary to introduce the adjoint eigenvalue problem, which reads as follows: Find $\lambda^* \in \mathbb{C}$ and a pair $(\mathbf{0}, 0) \neq (\boldsymbol{u}^*, p^*) \in \mathcal{X}$ such that

$$\left\{\begin{array}{rcll} a(\boldsymbol{v}, \boldsymbol{u}^*) - b(\boldsymbol{v}, p^*) & = & \overline{\lambda} c(\boldsymbol{v}, \boldsymbol{u}^*) & \forall \boldsymbol{v} \in \mathbf{H}_0^1(\Omega,\mathbb{C}), \\ -b(\boldsymbol{u}^*, q) & = & 0 & \forall q \in \mathrm{L}_0^2(\Omega,\mathbb{C}). \end{array}\right. \tag{2.8}$$

Now we introduce the adjoint of (2.5) defined by

$$\boldsymbol{T}^* : \mathbf{L}^2(\Omega,\mathbb{C}) \to \mathbf{L}^2(\Omega,\mathbb{C}), \qquad \boldsymbol{f} \mapsto \boldsymbol{T}^*\boldsymbol{f} := \widehat{\boldsymbol{u}}^*,$$

where $\widehat{\boldsymbol{u}}^* \in \mathbf{H}_0^1(\Omega,\mathbb{C})$ is the adjoint velocity of $\widehat{\boldsymbol{u}}$ and solves the following adjoint source problem: Find $(\widehat{\boldsymbol{u}}^*, \widehat{p}^*) \in \mathcal{X}$ such that

$$\left\{\begin{array}{rcll} a(\boldsymbol{v}, \widehat{\boldsymbol{u}}^*) - b(\boldsymbol{v}, \widehat{p}^*) & = & c(\boldsymbol{v}, \boldsymbol{f}) & \forall \boldsymbol{v} \in \mathbf{H}_0^1(\Omega,\mathbb{C}), \\ -b(\widehat{\boldsymbol{u}}^*, q) & = & 0 & \forall q \in \mathrm{L}_0^2(\Omega,\mathbb{C}). \end{array}\right. \tag{2.9}$$

Similar to Theorem 2.1, let us assume that the dual source and eigenvalue problems are such that the following estimate holds.

THEOREM 2.3. *There exist* $s^* > 0$ *such that for all* $\boldsymbol{f} \in \mathbf{L}^2(\Omega,\mathbb{C})$*, the solution* $(\widehat{\boldsymbol{u}}^*, \widehat{p}^*)$ *of problem* (2.9)*, satisfies* $\widehat{\boldsymbol{u}}^* \in \mathbf{H}^{1+s^*}(\Omega,\mathbb{C})$ *and* $\widehat{p}^* \in \mathrm{H}^{s^*}(\Omega,\mathbb{C})$*, and*

$$\|\widehat{\boldsymbol{u}}^*\|_{1+s^*,\Omega} + \|\widehat{p}^*\|_{s^*,\Omega} \leq C\|\boldsymbol{f}\|_{0,\Omega},$$

where $C > 0$ *is defined in Theorem* 2.1*. Further, if* $(\boldsymbol{u}^*, p^*)$ *is an eigenfunction satisfying* (2.8)*, then there exists* $r^* > 0$*, not necessarily equal to* s^**, such that* $(\boldsymbol{u}^*, p^*) \in \mathcal{X} \cap ((\mathbf{H}^{1+r^*}(\Omega,\mathbb{C}) \times \mathrm{H}^{r^*}(\Omega,\mathbb{C})))$ *and the following bound holds*

$$\|\widehat{\boldsymbol{u}}^*\|_{1+r^*,\Omega} + \|\widehat{p}^*\|_{r^*,\Omega} \leq C\|\widehat{\boldsymbol{u}}^*\|_{0,\Omega},.$$

Finally the spectral characterization of $\boldsymbol{T}^*$ is given as follows.

LEMMA 2.4. *(Spectral Characterization of $\boldsymbol{T}^*$). The spectrum of $\boldsymbol{T}^*$ is such that* $\text{sp}(\boldsymbol{T}^*) = \{0\} \cup \{\kappa_k^*\}_{k\in N}$ *where $\{\kappa_k^*\}_{k\in\mathbf{N}}$ is a sequence of complex eigenvalues that converge to zero, according to their respective multiplicities.*

It is easy to prove that if κ is an eigenvalue of $\boldsymbol{T}$ with multiplicity m, $\overline{\kappa^*}$ is an eigenvalue of $\boldsymbol{T}^*$ with the same multiplicity m.

Let us define the sesquilinear form $\widetilde{A} : \mathcal{X} \times \mathcal{X} \to \mathbb{C}$ by

$$\widetilde{A}((\boldsymbol{v}, q), (\boldsymbol{u}^*, p^*)) := a(\boldsymbol{v}, \boldsymbol{u}^*) - b(\boldsymbol{v}, p^*) + b(\boldsymbol{u}^*, q),$$

which allows us to rewrite the dual eigenvalue problem (2.8) as follows: Find $\lambda^* \in \mathbb{C}$ and the pair $(\mathbf{0}, 0) \neq (\boldsymbol{u}^*, p^*) \in \mathcal{X}$ such that

$$\widetilde{A}((\boldsymbol{v}, q), (\boldsymbol{u}^*, p^*)) = \lambda^* c(\boldsymbol{v}, \boldsymbol{u}^*) \quad \forall (\boldsymbol{v}, q) \in \mathcal{X}.$$

3. The virtual element method. In order to discretize the Oseen eigenvalue problem, we first go over nonconforming virtual element space in this section. The original purpose of this space's development was to approximate the Stokes equation numerically. In our research, we utilise the improved version created in [35].

3.1. Mesh notation and mesh regularity. We consider the family of meshes $\{\mathcal{T}_h\}_{h>0}$ such that each mesh $\mathcal{T}_h$ is a partition of the domain Ω into a finite collection of non-overlapping, polygonal elements K with mesh diameter h_K, and boundary ∂K. As usual, we define $h := \max_{K\in\mathcal{T}_h} h_K$. Furthermore, $\mathcal{E} := \mathcal{E}_{\text{int}} \cup \mathcal{E}_{\text{bdy}}$ denotes the set of mesh edges of $\mathcal{T}_h$ where $\mathcal{E}_{\text{int}}$ and $\mathcal{E}_{\text{bdy}}$ denotes respectively the subsets of the interior and boundary mesh edges.

Consider the polygonal element $K \in \mathcal{T}_h$. We denote the outward pointing normal and the tangent unit vector to the polygonal boundary ∂K by $\boldsymbol{n}_K$ and $\boldsymbol{t}_K$, respectively. For every edge $e \subset \partial K$, we denote by $\boldsymbol{n}_e$,and $\boldsymbol{t}_e$ the normal and tangent unit vectors to e, respectively. Conventionally, we assume that $\boldsymbol{n}_e$ points out of Ω if e is a boundary edge, and $\boldsymbol{n}_e$ and $\boldsymbol{t}_e$ form an anti-clockwise oriented pair along every internal edge e. Accordingly, it holds that $\boldsymbol{n}_e := (t_2, -t_1)$ whenever $\boldsymbol{t}_e := (t_1, t_2)$.

We define the space of piecewise polynomials of degree $k \geq 0$ by

$$\mathcal{P}_k(\mathcal{T}_h) := \{q \in \mathrm{L}^2(\Omega) : q|_K \in \mathcal{P}_k(K) \quad \forall K \in \mathcal{T}_h\}.$$

Similarly, for all integers $l > 0$, we define the broken Sobolev space of degree l on $\mathcal{T}_h$ of vector-valued fields, whose components are in $\mathbf{H}^l(K)$ for all mesh elements K, as

$$\mathbf{H}^l(\mathcal{T}_h) := \{\boldsymbol{\varphi} \in \mathbf{L}^2(\Omega) : \boldsymbol{\varphi}|_K \in \mathbf{H}^l(K) \quad \forall K \in \mathcal{T}_h\}.$$

We endow this functional space with the broken semi-norm

$$|\boldsymbol{\varphi}_h|_{1,h} := \Big(\sum_{K\in\mathcal{T}_h} |\boldsymbol{\varphi}|^2_{1,K} \Big)^{1/2}.$$

Consider the internal edge $e \subset \partial K^+ \cap \partial K^-$, where $K^+, K^- \in \mathcal{T}_h$, and $\boldsymbol{n}_e$ points from K^+ to K^-. We define the jump of a function $\boldsymbol{v}$ through e by $[\![\boldsymbol{v}]\!]|_e := \boldsymbol{v}|_{K^+} - \boldsymbol{v}|_K^-$ and, for boundary edges, we define $[\![\boldsymbol{v}]\!]|_e := \boldsymbol{v}|_e$. For the a priori error analysis, we need the following regularity assumptions on the mesh family $\{\mathcal{T}_h\}_{h>0}$.

ASSUMPTION 1. *(Mesh Regularity) There exists a positive constant $\sigma > 0$ such that for all $K \in \mathcal{T}_h$ it holds that*

- *(M1) the ratio between every edge length and the diameter h_K is bigger than σ;*
- *(M2) K is star-shaped with respect to a ball of radius ρ_K satisfying $\rho_K > \sigma h_K$.*

These mesh assumptions impose some constraints that are admissible for the formulation of the method discussed in the next subsection. In view of the following analysis, it is helpful to define the continuous bilinear forms $a(\cdot,\cdot)$, $b(\cdot,\cdot)$ and $c(\cdot,\cdot)$ on the discrete space $\mathbf{H}^1(\mathcal{T}_h)$ as a sum of local contributions.

$$
\begin{aligned}
a(\boldsymbol{w},\boldsymbol{v}) &:= \sum_{K\in\mathcal{T}_h} a^K_{\text{sym}}(\boldsymbol{w},\boldsymbol{v}) + a^K_{\text{skew}}(\boldsymbol{w},\boldsymbol{v}) \qquad \forall \boldsymbol{w},\boldsymbol{v}\in\mathbf{H}^1(\mathcal{T}_h),\\
b(\boldsymbol{v},q) &:= \sum_{K\in\mathcal{T}_h} b^K(\boldsymbol{v},q) \qquad \forall \boldsymbol{v}\in\mathbf{H}^1(\mathcal{T}_h) \text{ and } q\in \mathrm{L}^2_0(\Omega,\mathbb{C}),\\
c(\boldsymbol{w},\boldsymbol{v}) &:= \sum_{K\in\mathcal{T}_h} c^K(\boldsymbol{w},\boldsymbol{v}) \qquad \forall \boldsymbol{w},\boldsymbol{v}\in\mathbf{L}^2_0(\Omega,\mathbb{C}),\\
A((\boldsymbol{u},p),(\boldsymbol{v},q)) &:= \sum_{K\in\mathcal{T}_h} A^K((\boldsymbol{u},p),(\boldsymbol{v},q)) \qquad \forall (\boldsymbol{u},p),(\boldsymbol{v},q)\in\mathcal{X}.
\end{aligned}
$$

In the same way, we split elementwise the norm $\mathrm{L}^2(\Omega,\mathbb{C})$ by

$$
\|q\|_{0,\Omega} := \left(\sum_{K\in\mathcal{T}_h}\|q\|^2_{0,K}\right)^{1/2} \qquad \forall q\in\mathrm{L}^2(\Omega,\mathbb{C}).
$$

3.2. Local and global discrete space. In what follows we summarize the key ingredients for the discrete analysis, given by [35]. For $K\in\mathcal{T}_h$, we define the following auxiliary finite dimensional space

(3.1)
$$
\widetilde{\boldsymbol{\mathcal{S}}}(K) := \{\boldsymbol{v}\in\mathbf{H}^1(K) : \operatorname{div}\boldsymbol{v}\in\mathcal{P}_{k-1}(K), \operatorname{rot}\boldsymbol{v}\in\mathcal{P}_{k-1}(K), \boldsymbol{v}\cdot\boldsymbol{n}_e\in\mathcal{P}_k(e)\forall e\subset\partial K\}.
$$

We decompose the space $\widetilde{\boldsymbol{\mathcal{S}}}(K)$ in (3.1) into the direct sum of two subspace as follows

$$
\widetilde{\boldsymbol{\mathcal{S}}}(K) = \widetilde{\boldsymbol{\mathcal{S}}}_1(K)\oplus\widetilde{\boldsymbol{\mathcal{S}}}_0(K),
$$

where $\widetilde{\boldsymbol{\mathcal{S}}}_1(K) := \{\boldsymbol{v}\in\widetilde{\boldsymbol{\mathcal{S}}}(K) : \operatorname{div}\boldsymbol{v} = 0, \boldsymbol{v}\cdot\boldsymbol{n}_K|_{\partial K} = 0\}$ and

$$
\widetilde{\boldsymbol{\mathcal{S}}}_0(K) := \{\boldsymbol{v}\in\widetilde{\boldsymbol{\mathcal{S}}}(K) : \operatorname{rot}\boldsymbol{v} = 0\}. \tag{3.2}
$$

Additionally, we introduce the space

$$
\widetilde{\mathcal{H}} := \{\phi\in\mathrm{H}^2(K), \Delta^2\phi\in\mathcal{P}_{k-1}(K), \phi|_e = 0, \Delta\phi|_e\in\mathcal{P}_{k-1}(e)\forall e\subset\partial K\}. \tag{3.3}
$$

The local space is constructed as sum of (3.2), and curl of (3.3) as follows

$$
\widetilde{\boldsymbol{\mathcal{U}}} = \widetilde{\boldsymbol{\mathcal{S}}}_1(K)\oplus\mathbf{curl}\,\widetilde{\mathcal{H}}.
$$

We define the following operators:

- (H1) the edge polynomial moments:

$$
\frac{1}{|e|}\int_e \boldsymbol{v}\cdot\boldsymbol{n}_e q_k \quad \forall q_k\in\mathcal{P}_k(e), \forall e\subset\partial K;
$$

- (H2) the edge polynomial moments:

$$\frac{1}{|e|}\int_e \boldsymbol{v}\cdot\boldsymbol{t}_e q_{k-1} \quad \forall q_{k-1}\in\mathcal{P}_{k-1}(e), \forall e\subset\partial K;$$

- (H3) the elemental polynomial moments:

$$\frac{1}{|K|}\int_K \boldsymbol{v}\cdot\mathbf{q}_{k-2} \quad \forall \mathbf{q}_{k-2}\in\nabla\mathcal{P}_{k-1}(K);$$

- (H4) the elemental polynomial moments:

$$\frac{1}{|K|}\int_K \boldsymbol{v}\cdot\mathbf{q}_k^{\perp} \quad \forall \mathbf{q}_k^{\perp}\in(\nabla\mathcal{P}_{k+1}(K))^{\perp};$$

Here, $(\nabla\mathcal{P}_{k+1}(K))^{\perp}$ is the $\mathbf{L}^2$-orthogonal complement of $\nabla\mathcal{P}_{k+1}(K)$ in $\boldsymbol{\mathcal{P}}_k(K)$, where $\boldsymbol{\mathcal{P}}_k(K)$ is vector valued polynomial space on K of order k. Following [35], we deduce that the set of operators above provides a set of the degrees of freedom of the discrete space $\widetilde{\boldsymbol{\mathcal{U}}}$. Based on the computational aspect, we introduce the elliptic projection operator $\boldsymbol{\Pi}_K^{\nabla}:\widetilde{\boldsymbol{\mathcal{U}}}\to\boldsymbol{\mathcal{P}}_k(K)$:

$$\begin{aligned} &a_{\rm sym}(\boldsymbol{\Pi}_K^{\nabla}\boldsymbol{u},\mathbf{q}) = a_{\rm sym}(\boldsymbol{u},\mathbf{q}) \quad \forall \mathbf{q}\in\boldsymbol{\mathcal{P}}_k(K),\\ &\int_{\partial K}\boldsymbol{\Pi}_K^{\nabla}\boldsymbol{u}-\boldsymbol{u}=0. \end{aligned} \tag{3.4}$$

From the definition of the projection operator $\boldsymbol{\Pi}_K^{\nabla}$, we deduce the right-hand side of (3.4) are computable from (H1)-(H4). By employing the projection operator $\boldsymbol{\Pi}_K^{\nabla}$, we define a local computational space which is subspace of $\widetilde{\boldsymbol{\mathcal{U}}}$ as follows:

$$\begin{aligned}\boldsymbol{\mathcal{U}}(K) := \{\boldsymbol{v}\in\widetilde{\boldsymbol{\mathcal{U}}} : &\int_K(\boldsymbol{v}-\boldsymbol{\Pi}_K^{\nabla}\boldsymbol{v})\cdot\mathbf{q}_k = 0 \quad \forall \mathbf{q}_k\in(\nabla\mathcal{P}_{k+1}(K))^{\perp}/(\nabla\mathcal{P}_{k-1}(K))^{\perp}\\ \text{and}\quad &\int_e(\boldsymbol{v}-\boldsymbol{\Pi}_K^{\nabla}\boldsymbol{v})\cdot\boldsymbol{n}_e q_k = 0 \quad \forall q_k\in\mathcal{P}_k(e)/\mathcal{P}_{k-1}(e), \quad \forall e\subset\partial K\},\end{aligned}$$

where the symbol $\mathcal{V}/\mathcal{V}_1$ denotes the subspace of space $\mathcal{V}$ consisting of polynomials that are $\mathbf{L}^2(K)$-orthogonal to space $\mathcal{V}_1$. Since the projector $\boldsymbol{\Pi}_K^{\nabla}$ is invariant on polynomial function space $\boldsymbol{\mathcal{P}}_k(K)$, we deduce that $\boldsymbol{\mathcal{P}}_k(K)\subset\boldsymbol{\mathcal{U}}(K)$. Furthermore, (H1) and (H3) are a set of degrees of freedom for $\boldsymbol{\mathcal{U}}(K)$. For $K\in\mathcal{T}_h$, the local space $\boldsymbol{\mathcal{U}}(K)$ is unisolvent with respect to a certain set of bounded linear operators, which are defined as follows:

- the edge polynomial moments:

$$\frac{1}{|e|}\int_e \boldsymbol{v}\cdot\mathbf{q}_{k-1} \quad \forall \mathbf{q}_{k-1}\in\boldsymbol{\mathcal{P}}_{k-1}(e), \forall e\subset\partial K;$$

- the elemental polynomial moments

$$\frac{1}{|K|}\int_K \boldsymbol{v}\cdot\mathbf{q}_{k-2} \quad \forall \mathbf{q}_{k-2}\in\boldsymbol{\mathcal{P}}_{k-2}(K);$$

According to the definition of the virtual space $\boldsymbol{\mathcal{U}}(K)$, the term $\boldsymbol{\Pi}_K^{\nabla}\boldsymbol{v}$ is computable for all $\boldsymbol{v}\in\boldsymbol{\mathcal{U}}(K)$. Now we define the global nonconforming virtual space by

$$\boldsymbol{\mathcal{U}}_h := \Big\{\boldsymbol{v}\in\mathbf{L}^2(\Omega,\mathbb{C}) : \boldsymbol{v}|_K\in\boldsymbol{\mathcal{U}}(K)\forall K\in\mathcal{T}_h,\\ \int_e [\![\boldsymbol{v}]\!]_e\cdot\mathbf{q}_{k-1} = 0 \ \ \forall\mathbf{q}_{k-1}\in\boldsymbol{\mathcal{P}}_{k-1}(e)\forall e\in\mathcal{E}\Big\}.$$

Clearly the space $\boldsymbol{\mathcal{U}}_h$ is not continuous over Ω since $\boldsymbol{\mathcal{U}}_h\not\subset\mathbf{H}^1(\Omega)$. In the next lemma, we summarize two technical results that will be helpful in the derivation of the a priori estimates of the next sections. Further, we highlight that the $\mathbf{L}^2$ projection operator $\boldsymbol{\Pi}_K^0$ is computable on $\boldsymbol{\mathcal{U}}(K)$ [33]. To define the interpolation operator $\mathcal{I}$ on the space $\boldsymbol{\mathcal{U}}_h$, for each element $K\in\mathcal{T}_h$, we denote by Σ_i, the operator associated with the i-th local degree of freedom, $i=1,2,\ldots,N^{\mathrm{dof}}$. From the above construction, it is easily seen that for every smooth enough function $\boldsymbol{v}$, there exists an unique element $\mathcal{I}_K\boldsymbol{v}\in\boldsymbol{\mathcal{U}}_h(K)$ such that $\Sigma_i(\boldsymbol{v}-\mathcal{I}_K\boldsymbol{v})=0$, $\forall\ i=1,2,\ldots,N^{\mathrm{dof}}$. Then, we define the global interpolation $\mathcal{I}$ for $\boldsymbol{\mathcal{U}}_h$ by setting $\mathcal{I}|_K=\mathcal{I}_K\ \forall K\in\mathcal{T}_h$. Two technical conclusions that will be useful in deriving the a priori estimates of the following sections are summarized in the next lemma.

LEMMA 3.1. *The following statements hold:*

- *For each polygon $K\in\mathcal{T}_h$ and any t such that $1\le t\le k+1$, it holds that*

$$\|\boldsymbol{v}-\mathcal{I}_K\boldsymbol{v}\|_{m,K}\le Ch^{t-m}|\boldsymbol{v}|_{t,K}\qquad m=0,1. \tag{3.5}$$

- *For each polygon $K\in\mathcal{T}_h$ and any t such that $1\le t\le k+1$, there exists a polynomial $\boldsymbol{v}_\pi\in\boldsymbol{\mathcal{P}}_k(K)$, such that*

$$\|\boldsymbol{v}-\boldsymbol{v}_\pi\|_{m,K}\le Ch^{t-m}|\boldsymbol{v}|_{t,K}\qquad m=0,1. \tag{3.6}$$

On the other hand, the discrete pressure space is given by

$$\mathrm{Q}_h := \{q_h\in\mathrm{L}^2(\Omega,\mathbb{C})\,:\,q_h|_K\in\mathcal{P}_{k-1}(K),\quad\forall K\in\mathcal{T}_h\},$$

We also introduce the L^2-orthogonal projection $\mathcal{R}_h:\mathrm{L}^2(\Omega)\to\mathrm{Q}_h$ and the following approximation result holds for $0\le t\le 1$ (see [12] for instance)

$$\|q-\mathcal{R}_hq\|_{0,\Omega}\le Ch^t\|q\|_{s,\Omega},\qquad\forall q\in\mathrm{H}^t(\Omega). \tag{3.7}$$

Let us introduce the operator $\mathrm{div}_h(\cdot)$ which corresponds to the discretized global form of the divergence operator, i.e., $(\mathrm{div}_h\,\boldsymbol{v})|_K=\mathrm{div}(\boldsymbol{v}|_K)$ for all $K\in\mathcal{T}_h$ (and sufficiently regular $\boldsymbol{v}$). From the above construction, we deduce that $\mathrm{div}_h\boldsymbol{\mathcal{U}}_h\subset\mathrm{Q}_h$, and the relation between the virtual interpolation operator and $\mathcal{R}_h$ is as follows $\mathrm{div}_h\,\mathcal{I}\boldsymbol{v}=\mathcal{R}_h\,\mathrm{div}_h\,\boldsymbol{v}$ for all $\boldsymbol{v}\in\mathbf{H}^1(\Omega)$. Now, let $S^K(\cdot,\cdot)$ be any symmetric positive definite bilinear form chosen to satisfy

$$c_0a_{\mathrm{sym}}^K(\boldsymbol{v}_h,\boldsymbol{v}_h)\le S^K(\boldsymbol{v}_h,\boldsymbol{v}_h)\le c_1a_{\mathrm{sym}}^K(\boldsymbol{v}_h,\boldsymbol{v}_h), \tag{3.8}$$

for some positive constants c_0 and c_1 depending only on the constant σ from the mesh assumptions $M1$ and $M2$. Then, for all $\boldsymbol{w}_h,\boldsymbol{v}_h\in\boldsymbol{\mathcal{U}}_h$, we introduce on each element K the local (and computable) bilinear forms

$$a_{h,\mathrm{sym}}^K(\boldsymbol{w}_h,\boldsymbol{v}_h) := a_{\mathrm{sym}}^K(\boldsymbol{\Pi}_K^{\nabla}\boldsymbol{w}_h,\boldsymbol{\Pi}_K^{\nabla}\boldsymbol{v}_h)+S^K(\boldsymbol{w}_h-\boldsymbol{\Pi}_K^{\nabla}\boldsymbol{w}_h,\boldsymbol{v}_h-\boldsymbol{\Pi}_K^{\nabla}\boldsymbol{v}_h);$$

$$a_{h,\mathrm{skew}}^K(\boldsymbol{w}_h,\boldsymbol{v}_h) := \frac{1}{2}\int_K\left(\left(\boldsymbol{\beta}\cdot\boldsymbol{\Pi}_{k-1,K}^0\nabla\right)\boldsymbol{w}_h\cdot\boldsymbol{\Pi}_K^0\boldsymbol{v}_h-\left(\boldsymbol{\beta}\cdot\boldsymbol{\Pi}_{k-1,K}^0\nabla\right)\boldsymbol{v}_h\cdot\boldsymbol{\Pi}_K^0\boldsymbol{w}_h\right);$$

$$c_h^K(\boldsymbol{w},\boldsymbol{v}) := c^K(\boldsymbol{\Pi}_K^0\boldsymbol{w}_h,\boldsymbol{\Pi}_K^0\boldsymbol{v}_h).$$

The construction of $a_{h,\mathrm{sym}}^K(\cdot,\cdot)$ and $c_h^K(\cdot,\cdot)$ guarantees the usual consistency and stability properties of the VEM. With this considerations at hand, the following result holds true which is direct from [11].

Lemma 3.2. *The local bilinear forms $a_{h,sym}^K(\cdot,\cdot)$ and $c_h^K(\cdot,\cdot)$ on each element K satisfy:*

- *Consistency: for all $h>0$ and for all $K\in\mathcal{T}_h$ we have that*

$$a_{h,sym}^K(\boldsymbol{v}_h,\mathbf{q}_k)=a_{sym}^K(\boldsymbol{v}_h,\mathbf{q}_k)\qquad\forall\mathbf{q}_k\in\boldsymbol{\mathcal{P}}_k(K),$$
$$c_h^K(\boldsymbol{v}_h,\mathbf{q}_k)=c^K(\boldsymbol{v}_h,\mathbf{q}_k)\qquad\forall\mathbf{q}_k\in\boldsymbol{\mathcal{P}}_k(K).$$

- *Stability: for all $K\in\mathcal{T}_h$, there exist positive constants c_*, c^* and d^*, independent of h, such that*

$$c_*a_{sym}^K(\boldsymbol{v}_h,\boldsymbol{v}_h)\leq a_{h,sym}^K(\boldsymbol{v}_h,\boldsymbol{v}_h)\leq c^*a_{sym}^K(\boldsymbol{v}_h,\boldsymbol{v}_h)\qquad\forall\boldsymbol{v}_h\in\boldsymbol{\mathcal{U}}_h,$$
$$c_h^K(\boldsymbol{v}_h,\boldsymbol{v}_h)\leq d^*c^K(\boldsymbol{v}_h,\boldsymbol{v}_h)\qquad\forall\boldsymbol{v}_h\in\boldsymbol{\mathcal{U}}_h.$$

For the bilinear form $b_h(\cdot,\cdot)$, we do not introduce any approximation and simply set

$$b_h(\boldsymbol{v}_h,q_h):=\sum_{K\in\mathcal{T}_h}b^K(\boldsymbol{v}_h,q_h)=-\sum_{K\in\mathcal{T}_h}\int_K q_h\operatorname{div}\boldsymbol{v}_h,\qquad\forall\boldsymbol{v}_h\in\boldsymbol{\mathcal{U}}_h,q_h\in\mathrm{Q}_h.$$

Since $b_h(\boldsymbol{v}_h,q_h)$ is computable in each element $K\in\mathcal{T}_h$ with the aid of the degrees of freedom defined on $\boldsymbol{\mathcal{U}}(K)$. Naturally for all $\boldsymbol{w}_h,\boldsymbol{v}_h\in\boldsymbol{\mathcal{U}}_h$ we can introduce the following bilinear form

$$a_h(\boldsymbol{w}_h,\boldsymbol{v}_h):=\sum_{K\in\mathcal{T}_h}a_h^K(\boldsymbol{w}_h,\boldsymbol{v}_h)=\sum_{K\in\mathcal{T}_h}a_{h,\mathrm{sym}}^K(\boldsymbol{w}_h,\boldsymbol{v}_h)+a_{h,\mathrm{skew}}^K(\boldsymbol{w}_h,\boldsymbol{v}_h).$$

It is easy to check that $a_h(\cdot,\cdot)$ and $b_h(\cdot,\cdot)$ are continuous sesquilinear forms. Indeed, for $a_h(\cdot,\cdot)$ we have

$$|a_h(\boldsymbol{u}_h,\boldsymbol{v}_h)|\leq|a_{h,\mathrm{sym}}(\boldsymbol{u}_h,\boldsymbol{v}_h)|+|a_{h,\mathrm{skew}}(\boldsymbol{u}_h,\boldsymbol{v}_h)|,\tag{3.9}$$

where we need to estimate each contribution on the right hand side of the inequality above. For the symmetric part we have

$$\begin{aligned}|a_{h,\mathrm{sym}}(\boldsymbol{u}_h,\boldsymbol{v}_h)|&=\left|\sum_{K\in\mathcal{T}_h}a_{\mathrm{sym}}^K(\boldsymbol{u}_h,\boldsymbol{v}_h)+S^K(\boldsymbol{u}_h-\boldsymbol{\Pi}_K^\nabla\boldsymbol{u}_h,\boldsymbol{v}_h-\boldsymbol{\Pi}_K^\nabla\boldsymbol{v}_h)\right|\\&\leq\sum_{K\in\mathcal{T}_h}\nu\|\nabla\boldsymbol{\Pi}_K^\nabla\boldsymbol{u}_h\|_{0,K}\|\nabla\boldsymbol{\Pi}_K^\nabla\boldsymbol{v}_h\|_{0,K}+c_1\nu\|\nabla(\boldsymbol{\Pi}_K^\nabla\boldsymbol{u}_h-\boldsymbol{u}_h)\|_{0,K}\|\nabla(\boldsymbol{\Pi}_K^\nabla\boldsymbol{v}_h-\boldsymbol{v}_h)\|_{0,K}\\&\leq\nu\max\{\widetilde{c}_1,1\}\|\boldsymbol{u}_h\|_{1,h}\|\boldsymbol{v}_h\|_{1,h},\end{aligned}\tag{3.10}$$

where the constant $\widetilde{c}_1$ is the sum of all the constants c_1 involved in (3.8) for each element $K\in\mathcal{T}_h$. Now, for the skew-symmetric part we have

$$
\begin{aligned}
(3.11)\quad |a_{h,\text{skew}}(\boldsymbol{u}_h,\boldsymbol{v}_h)| &\le \frac{1}{2}\left|\sum_{K\in\mathcal{T}_h}\int_K(\boldsymbol{\beta}\cdot\boldsymbol{\Pi}^0_{k-1,K})\boldsymbol{u}_h\boldsymbol{\Pi}^0_{k,K}\boldsymbol{v}_h\right| \\
&\quad+\frac{1}{2}\left|\sum_{K\in\mathcal{T}_h}\int_K(\boldsymbol{\beta}\cdot\boldsymbol{\Pi}^0_{k-1,K})\boldsymbol{v}_h\boldsymbol{\Pi}^0_{k,K}\boldsymbol{u}_h\right| \\
&\le \frac{1}{2}\sum_{K\in\mathcal{T}_h}\|\boldsymbol{\beta}\|_{\infty,K}\|\boldsymbol{\Pi}^0_{k-1,K}\nabla\boldsymbol{u}_h\|_{0,\varepsilon}\|\boldsymbol{\Pi}^0_{k,K}\boldsymbol{v}_h\|_{0,K} \\
&\quad+\frac{1}{2}\sum_{K\in\mathcal{T}_h}\|\boldsymbol{\beta}\|_{\infty,K}\|\boldsymbol{\Pi}^0_{k-1,K}\nabla\boldsymbol{v}_h\|_{0,K}\|\boldsymbol{\Pi}^0_{k,K}\boldsymbol{u}_h\|_{0,K} \\
&\le \|\boldsymbol{\beta}\|_{\infty,\Omega}C_{\text{I}}C_{\text{II}}\|\boldsymbol{u}_h\|_{1,h}\|\boldsymbol{v}_h\|_{1,h},
\end{aligned}
$$

where $C_{\text{I}},C_{\text{II}}>0$ are the stability constants of $\boldsymbol{\Pi}^0_{k-1,K}$ and $\boldsymbol{\Pi}^0_{k,K}$, respectively. Hence, replacing (3.10) and (3.11) in (3.9) we have that

$$|a_h(\boldsymbol{u}_h,\boldsymbol{v}_h)|\le\max\{\nu\max\{\widetilde{c}_1,1\},\|\boldsymbol{\beta}\|_{\infty,\Omega}C_{\text{I}}C_{\text{II}}\}\|\boldsymbol{u}_h\|_{1,h}\|\boldsymbol{v}_h\|_{1,h},$$

which proves the boundedness of $a_h(\cdot,\cdot)$. On the other hand, for $b_h(\cdot,\cdot)$ we have

$$
\begin{aligned}
|b_h(\boldsymbol{v}_h,q_h)| = \left|\sum_{K\in\mathcal{T}_h}\int_K q_h\operatorname{div}\boldsymbol{v}_h\right| &\le \sum_{K\in\mathcal{T}_h}\|q_h\|_{0,K}\|\operatorname{div}\boldsymbol{v}_h\|_{0,K} \\
&\le \sum_{K\in\mathcal{T}_h}\|q_h\|_{0,K}\|\nabla\boldsymbol{v}_h\|_{0,K}\le\|q_h\|_{0,\Omega}\|\boldsymbol{v}_h\|_{1,h},
\end{aligned}
$$

proving that $b_h(\cdot,\cdot)$ is also continuous.

3.3. The discrete eigenvalue problem. The nonconforming virtual element discretization of the variational formulation (2.3) reads as follows. Find $\lambda\in\mathbb{C}$ and $(\boldsymbol{0},0)\neq(\boldsymbol{u}_h,p_h)\in\mathcal{X}_h$ such that

$$
(3.12)\qquad \left\{\begin{array}{rcll} a_h(\boldsymbol{u}_h,\boldsymbol{v}_h)+b_h(\boldsymbol{v}_h,p_h) &=& \lambda_h c_h(\boldsymbol{u}_h,\boldsymbol{v}_h) & \forall\boldsymbol{v}_h\in\boldsymbol{\mathcal{U}}_h,\\ b_h(\boldsymbol{u}_h,q_h) &=& 0 & \forall q_h\in\mathrm{Q}_h,\end{array}\right.
$$

where $\mathcal{X}_h:=\boldsymbol{\mathcal{U}}_h\times\mathrm{Q}_h$. Thanks to the stability of the bilinear form $a^K_{h,\text{sym}}(\cdot,\cdot)$ and the definition of the bilinear form $a^K_{h,\text{skew}}(\cdot,\cdot)$, it is easy to check that $a_h(\cdot,\cdot)$ is coercive, i.e.

$$c|\boldsymbol{v}_h|^2_{1,h}\le a_h(\boldsymbol{v}_h,\boldsymbol{v}_h)\qquad\forall\boldsymbol{v}_h\in\boldsymbol{\mathcal{U}}_h.$$

On the other hand, given the discrete spaces $\boldsymbol{\mathcal{U}}_h$ and Q_h , satisfy that $\operatorname{div}_h\boldsymbol{\mathcal{U}}_h\subset\mathrm{Q}_h$, standard arguments (see [18]) guarantee that there exists a positive β_0, independent of h, such that

$$(3.13)\qquad \sup_{\boldsymbol{v}_h\in\boldsymbol{\mathcal{U}}_h}\frac{b_h(\boldsymbol{v}_h,q_h)}{|\boldsymbol{v}_h|_{1,h}}\ge\beta_0\|q_h\|_{0,\Omega}\quad\forall q_h\in\mathrm{Q}_h.$$

The next step is to introduce the discrete solution operator $\boldsymbol{T}_h:\mathbf{L}^2(\Omega)\to\boldsymbol{\mathcal{U}}_h\subset\mathbf{L}^2(\Omega)$, defined by $\boldsymbol{T}_h\boldsymbol{f}:=\widehat{\boldsymbol{u}}_h$, where $\widehat{\boldsymbol{u}}_h$ is the solution of the corresponding discrete source problem:

$$\text{(3.14)}\qquad \left\{\begin{array}{rcll} a_h(\widehat{\boldsymbol{u}}_h,\boldsymbol{v}_h)+b_h(\boldsymbol{v}_h,\widehat{p}_h) &=& c_h(\boldsymbol{f},\boldsymbol{v}_h) & \forall \boldsymbol{v}_h\in\boldsymbol{\mathcal{U}}_h,\\ b_h(\widehat{\boldsymbol{u}}_h,q_h) &=& 0 & \forall q_h\in \mathrm{Q}_h. \end{array}\right.$$

Since the discrete inf-sup condition is satisfied, the operator $\boldsymbol{T}_h$ is well defined. Moreover, we have the following stability result.

$$\nu|\widehat{\boldsymbol{u}}_h|_{1,h}\leq C_p\|\boldsymbol{f}\|_{0,\Omega},$$

whereas for the pressure we have

$$\|\widehat{p}_h\|_{0,\Omega}\leq \frac{1}{\beta}\left(C_p\|\boldsymbol{f}\|_{0,\Omega}+\nu^{1/2}|\widehat{\boldsymbol{u}}_h|_{1,h}\left(\nu^{1/2}+\frac{C_p\|\boldsymbol{\beta}\|_{\infty,\Omega}}{\nu^{1/2}}\right)\right).$$

As in the continuous case, we have the following relation between the discrete spectral problem and its source problem, i.e., $(\lambda_h,(\boldsymbol{u}_h,p_h))$ is a solution of Problem (3.12) if and only if $(\kappa_h,\boldsymbol{u}_h)$ is an eigenpair of $\boldsymbol{T}_h$, i.e., $\boldsymbol{T}_h\boldsymbol{u}_h=\kappa_h\boldsymbol{u}_h$ with $\kappa_h=1/\lambda_h$ and $\lambda_h\neq 0$. The discrete version of the spectral problem (2.7) is written as

Problem 3.3. *Find* $(\lambda_h,\boldsymbol{u}_h,p_h)\in\mathbb{R}\times\boldsymbol{\mathcal{U}}_h\times\mathrm{Q}_h$ *such that* $\|\boldsymbol{u}_h\|_{0,\Omega}+\|p_h\|_{0,\Omega}>0$, *and*

$$A_h((\boldsymbol{u}_h,p_h),(\boldsymbol{v}_h,q_h))=\lambda_h c_h(\boldsymbol{u}_h,\boldsymbol{v}_h),\quad \forall(\boldsymbol{v}_h,q_h)\in\boldsymbol{\mathcal{U}}_h\times\mathrm{Q}_h,$$

where

$$A_h((\boldsymbol{u}_h,p_h),(\boldsymbol{v}_h,q_h))=a_h(\boldsymbol{u}_h,\boldsymbol{v}_h)+b_h(\boldsymbol{v}_h,p_h)-b_h(\boldsymbol{u}_h,q_h).$$

In Problem 3.3, $A_h(\cdot,\cdot)$, and $c_h(\cdot,\cdot)$ are the virtual element discretization of $A(\cdot,\cdot)$, and $c(\cdot,\cdot)$ respectively, whereas $(\lambda_h,(\boldsymbol{u}_h,p_h))$ is the virtual element approximation of the continuous solution $(\lambda,(\boldsymbol{u},p))$. For the exposition's sake, we first introduce the basic notation and the few mesh regularity assumptions that we need for the convergence analysis of the virtual element approximation of the next section. Likewise, we define the discrete formulation corresponding to the adjoint problem, i.e. Eqn. (2.8). The identical arguments as for the primal formulation imply the well-posedness of the discrete formulation.

Remark 3.4. The discrete bilinear form $c_h(\cdot,\cdot)$ is defined neglecting the corresponding stabilizer. We emphasize that we define the solution operator on $\mathbf{L}^2$ which does not guarantee the existence of the trace on the boundary, and consequently, the edge momentum will not be well-defined. This does not guarantee the existence of the associated stabilizer. However, the proposed definition $c_h(\cdot,\cdot)$ needs only $\mathbf{L}^2$ regularity and hence suitable for our strategy.

As the case continues, it is now necessary to define the adjoint discrete problem, which consists in: Find $\lambda^*\in\mathbb{C}$ and $(\mathbf{0},0)\neq(\boldsymbol{u}_h^*,p_h^*)\in\mathcal{X}_h$ such that

$$\text{(3.15)}\qquad \left\{\begin{array}{rcll} a_h(\boldsymbol{v}_h,\boldsymbol{u}_h^*)-b_h(\boldsymbol{v}_h,p_h^*) &=& \overline{\lambda_h^*}c_h(\boldsymbol{v}_h,\boldsymbol{u}_h^*) & \forall \boldsymbol{v}_h\in\boldsymbol{\mathcal{U}}_h,\\ -b_h(\boldsymbol{u}_h^*,q_h) &=& 0 & \forall q_h\in \mathrm{Q}_h, \end{array}\right.$$

Now we define the discrete version of the operator $\boldsymbol{T}^*$ is then given by $\boldsymbol{T}_h^*:\mathbf{L}^2(\Omega)\to\boldsymbol{\mathcal{U}}_h\subset\mathbf{L}^2(\Omega)$, defined by $\boldsymbol{T}_h^*\boldsymbol{f}:=\widehat{\boldsymbol{u}}_h^*$, where $\widehat{\boldsymbol{u}}_h^*$ is the solution of the corresponding discrete source problem:

$$\text{(3.16)}\qquad \left\{\begin{array}{rcll} a_h(\boldsymbol{v}_h,\widehat{\boldsymbol{u}}_h^*)-b_h(\boldsymbol{v}_h,\widehat{p}_h^*) &=& c_h(\boldsymbol{v}_h,\boldsymbol{f}) & \forall \boldsymbol{v}_h\in\boldsymbol{\mathcal{U}}_h,\\ -b_h(\widehat{\boldsymbol{u}}_h,q_h) &=& 0 & \forall q_h\in \mathrm{Q}_h. \end{array}\right.$$

4. A priori error estimates for the source problem. We are now in a position to be able to show that $\boldsymbol{T}_h$ converges to $\boldsymbol{T}$ as h becomes zero in the broken norm. This is contained in the following result

THEOREM 4.1. *Let $\boldsymbol{f} \in \mathbf{L}^2(\Omega,\mathbb{C})$ be such that $\widehat{\boldsymbol{u}} := \boldsymbol{T}\boldsymbol{f}$ and $\widehat{\boldsymbol{u}}_h := \boldsymbol{T}_h\boldsymbol{f}$ with $\widehat{\boldsymbol{u}} \in \mathbf{H}^{1+s}(\Omega,\mathbb{C})$, $s \geq 1$. Then, there exists a positive constant C, independent of h, such that*

$$\|(\boldsymbol{T}-\boldsymbol{T}_h)\boldsymbol{f}\|_{1,h} = \|\widehat{\boldsymbol{u}}-\widehat{\boldsymbol{u}}_h\|_{1,h} \leq Ch^{\min\{k,s\}}\Big(|\widehat{\boldsymbol{u}}|_{1+s,\Omega} + |\widehat{p}|_{s,\Omega} + \|\boldsymbol{f}\|_{s-1,\Omega}\Big).$$

where C is a positive constant independent of h.

Proof. By employing the interpolation operator on the discrete space, i.e., $\mathcal{I}$, we split the difference $\widehat{\boldsymbol{u}}-\widehat{\boldsymbol{u}}_h = \widehat{\boldsymbol{u}}-\mathcal{I}\widehat{\boldsymbol{u}}+\mathcal{I}\widehat{\boldsymbol{u}}-\widehat{\boldsymbol{u}}_h$. An application of the approximation properties of the interpolation operator yields the bound of $\boldsymbol{\eta}_h = \widehat{\boldsymbol{u}}-\mathcal{I}\widehat{\boldsymbol{u}}$. To estimate the other term, i.e., $\boldsymbol{\delta}_h := \mathcal{I}\widehat{\boldsymbol{u}}-\widehat{\boldsymbol{u}}_h$, we apply the coercivity and the fact that $\operatorname{div}(\mathcal{I}\widehat{\boldsymbol{u}}-\widehat{\boldsymbol{u}}_h) = 0$ (see [35]) in order to obtain

$$\begin{aligned}
(4.1)\quad C_\alpha\ \|\boldsymbol{\delta}_h\|_{1,h}^2 &\leq a_h(\mathcal{I}\widehat{\boldsymbol{u}},\boldsymbol{\delta}_h) - a_h(\widehat{\boldsymbol{u}}_h,\boldsymbol{\delta}_h)\\
&= a_h(\mathcal{I}\widehat{\boldsymbol{u}},\boldsymbol{\delta}_h) - c_h(\boldsymbol{f},\boldsymbol{\delta}_h) + b_h(\boldsymbol{\delta}_h,\widehat{p}_h) - b_h(\widehat{\boldsymbol{u}}_h,q_h) = a_h(\mathcal{I}\widehat{\boldsymbol{u}},\boldsymbol{\delta}_h) - c_h(\boldsymbol{f},\boldsymbol{\delta}_h)\\
&= a_{h,\text{skew}}(\mathcal{I}\widehat{\boldsymbol{u}},\boldsymbol{\delta}_h) + a_{h,\text{sym}}(\mathcal{I}\widehat{\boldsymbol{u}}-\boldsymbol{u}_\pi,\boldsymbol{\delta}_h) + a_{\text{sym}}(\widehat{\boldsymbol{u}}_\pi-\widehat{\boldsymbol{u}},\boldsymbol{\delta}_h) + a_{\text{sym}}(\widehat{\boldsymbol{u}},\boldsymbol{\delta}_h) - c_h(\boldsymbol{f},\boldsymbol{\delta}_h)\\
&= \underbrace{a_{h,\text{skew}}(\mathcal{I}\widehat{\boldsymbol{u}},\boldsymbol{\delta}_h) - a_{\text{skew}}(\widehat{\boldsymbol{u}},\boldsymbol{\delta}_h)}_{A_1} + \underbrace{a_{h,\text{sym}}(\mathcal{I}\widehat{\boldsymbol{u}}-\boldsymbol{u}_\pi,\boldsymbol{\delta}_h) + a_{\text{sym}}(\widehat{\boldsymbol{u}}_\pi-\boldsymbol{u},\boldsymbol{\delta}_h)}_{A_2}\\
&\qquad + \underbrace{c(\boldsymbol{f},\boldsymbol{\delta}_h) - c_h(\boldsymbol{f},\boldsymbol{\delta}_h)}_{A_3} + \underbrace{\boldsymbol{\mathcal{N}}_h((\widehat{\boldsymbol{u}},\widehat{p}),\boldsymbol{\delta}_h)}_{A_4}.
\end{aligned}$$

By using the approximation properties of the interpolation operator and polynomial representative, we bound the each of (4.1). $\boldsymbol{\mathcal{N}}_h((\widehat{\boldsymbol{u}},\widehat{p}),\boldsymbol{\delta}_h)$ is the consistency error appeared due to non-conforming approximation of the discrete space. In order to estimate the Term A_1, first we note that

$$(4.2)\qquad A_1 = \sum_{K\in\mathcal{T}_h}\left(\underbrace{a^K_{\text{skew}}(\mathcal{I}\widehat{\boldsymbol{u}}-\widehat{\boldsymbol{u}},\boldsymbol{\delta}_h)}_{B_1} + \underbrace{a^K_{h,\text{skew}}(\mathcal{I}\widehat{\boldsymbol{u}},\boldsymbol{\delta}_h) - a^K_{\text{skew}}(\mathcal{I}\widehat{\boldsymbol{u}},\boldsymbol{\delta}_h)}_{B_2}\right).$$

Now, to estimate B_1, using Lemma 3.1, we derive as follow.

$$\begin{aligned}
a^K_{\text{skew}}(\mathcal{I}\widehat{\boldsymbol{u}}-\widehat{\boldsymbol{u}},\boldsymbol{\delta}_h)| &\leq C\left(\|\boldsymbol{\beta}\|_{\infty,K}\|\mathcal{I}\widehat{\boldsymbol{u}}-\widehat{\boldsymbol{u}}\|_{1,K}\|\boldsymbol{\delta}_h\|_{1,K}\right)\\
&\leq Ch_K^{\min\{s,k\}}\|\boldsymbol{\beta}\|_{\infty,K}|\boldsymbol{u}|_{1+s,K}\|\boldsymbol{\delta}_h\|_{1,K}.
\end{aligned}$$

To estimate B_2, is necessary to note that for each $K \in \mathcal{T}_h$, $\boldsymbol{u},\boldsymbol{v} \in \mathbf{H}^1(K)$ and $\boldsymbol{\beta} \in \mathbf{L}^\infty(K)$, we have:

$$\int_K (\boldsymbol{\beta}\cdot\nabla)\boldsymbol{u}\cdot\boldsymbol{v} = \int_K (\nabla\boldsymbol{u})\boldsymbol{\beta}\cdot\boldsymbol{v} = \int_K \nabla\boldsymbol{u} : (\boldsymbol{\beta}\otimes\boldsymbol{v})^{\mathtt{t}}.$$

For each polygon $K \in \mathcal{T}_h$, employing the orthogonality property of the $\mathbf{L}^2$ projection operator, we obtain

$$\begin{aligned}&\int_K \Big((\boldsymbol{\Pi}^0_{k-1,K}(\nabla\mathcal{I}\widehat{\boldsymbol{u}}))\boldsymbol{\beta}\cdot\boldsymbol{\Pi}^0_K\boldsymbol{\delta}_h-(\nabla\mathcal{I}\widehat{\boldsymbol{u}})\boldsymbol{\beta}\cdot\boldsymbol{\delta}_h\Big)\\&=\int_K\Big(\big(\boldsymbol{\Pi}^0_{k-1,K}(\nabla\mathcal{I}\widehat{\boldsymbol{u}})-\nabla\mathcal{I}\widehat{\boldsymbol{u}}\big):(\boldsymbol{\beta}\otimes(\boldsymbol{\Pi}^0_K\boldsymbol{\delta}_h-\boldsymbol{\delta}_h))^{\mathtt{t}}\\&\quad+\int_K\big(\boldsymbol{\Pi}^0_{k-1,K}(\nabla\mathcal{I}\widehat{\boldsymbol{u}})-\nabla\mathcal{I}\widehat{\boldsymbol{u}}\big):\big((\boldsymbol{\beta}\otimes\boldsymbol{\delta}_h)^{\mathtt{t}}-\boldsymbol{\Pi}^0_{k-1,K}((\boldsymbol{\beta}\otimes\boldsymbol{\delta}_h)^{\mathtt{t}})\big)\\&\quad+\int_K\big((\nabla\mathcal{I}\widehat{\boldsymbol{u}})\boldsymbol{\beta}-\boldsymbol{\Pi}^0_K((\nabla\mathcal{I}\widehat{\boldsymbol{u}})\boldsymbol{\beta})\big)\cdot(\boldsymbol{\Pi}^0_K\boldsymbol{\delta}_h-\boldsymbol{\delta}_h).\end{aligned}$$

Now assuming that $\nabla\widehat{\boldsymbol{u}}\in\mathbf{H}^s(K)$, $\boldsymbol{\beta}\in\mathbf{W}^{1,\infty}(K)$ and $\boldsymbol{\delta}_h\in\mathbf{H}^1(K)$ and approximation properties of $\boldsymbol{\Pi}^0_K$, continuity of $\mathbf{L}^2$ inner product, it follows that :

$$\begin{aligned}&\int_K\Big(\boldsymbol{\beta}\cdot\boldsymbol{\Pi}^0_{k-1,K}(\nabla\mathcal{I}\widehat{\boldsymbol{u}})\cdot\boldsymbol{\Pi}^0_K\boldsymbol{\delta}_h-\boldsymbol{\beta}\cdot(\nabla\mathcal{I}\widehat{\boldsymbol{u}})\cdot\boldsymbol{\delta}_h\Big)\\&\leq\|\boldsymbol{\Pi}^0_{k-1,K}(\nabla\mathcal{I}\widehat{\boldsymbol{u}})-\nabla\mathcal{I}\widehat{\boldsymbol{u}}\|_{0,K}\|\boldsymbol{\beta}\otimes(\boldsymbol{\Pi}^0_K\boldsymbol{\delta}_h-\boldsymbol{\delta}_h)^{\mathtt{t}}\|_{0,K}\\&\quad+\|\boldsymbol{\Pi}^0_{k-1,K}(\nabla\mathcal{I}\widehat{\boldsymbol{u}})-\nabla\mathcal{I}\widehat{\boldsymbol{u}}\|_{0,K}\|(\boldsymbol{\beta}\otimes\boldsymbol{\delta}_h)^{\mathtt{t}}-\boldsymbol{\Pi}^0_{k-1,K}((\boldsymbol{\beta}\otimes\boldsymbol{\delta}_h)^{\mathtt{t}})\|_{0,K}\\&\quad+\|(\nabla\mathcal{I}\widehat{\boldsymbol{u}})\boldsymbol{\beta}-\boldsymbol{\Pi}^0_K((\nabla\mathcal{I}\widehat{\boldsymbol{u}})\boldsymbol{\beta})\|_{0,K}\|\boldsymbol{\Pi}^0_K\boldsymbol{\delta}_h-\boldsymbol{\delta}_h\|_{0,K}\\&\leq Ch_K^{\min\{s,k\}}\|\boldsymbol{\beta}\|_{\mathbf{W}^{1,\infty}(K)}|\widehat{\boldsymbol{u}}|_{1+s,K}|\boldsymbol{\delta}_h|_{1,K}.\end{aligned}\tag{4.3}$$

Borrowing the analogous arguments as previous estimate, we obtain:

$$\int_K\Big(\boldsymbol{\Pi}^0_{k-1,K}(\nabla\boldsymbol{\delta}_h)\boldsymbol{\beta}\cdot\boldsymbol{\Pi}^0_K\mathcal{I}\widehat{\boldsymbol{u}}-(\nabla\boldsymbol{\delta}_h)\boldsymbol{\beta}\cdot\mathcal{I}\widehat{\boldsymbol{u}}\Big)\leq C(\boldsymbol{\beta})h_K^{\min\{s,k\}}|\widehat{\boldsymbol{u}}|_{1+s,K}|\boldsymbol{\delta}_h|_{1,K}.\tag{4.4}$$

Thus, from the two estimates above ((4.3), (4.4)), it is obtained that

$$B_2\leq Ch_K^{\min\{s,k\}}\|\boldsymbol{\beta}\|_{\mathbf{W}^{1,\infty}(K)}|\widehat{\boldsymbol{u}}|_{1+s,K}|\boldsymbol{\delta}_h|_{1,K},$$

and finally considering the sum over all elements K

$$A_1\leq Ch^{\min\{s,k\}}\|\boldsymbol{\beta}\|_{\mathbf{W}^{1,\infty}(\Omega)}|\widehat{\boldsymbol{u}}|_{1+s,\Omega}|\boldsymbol{\delta}_h|_{1,h}.\tag{4.5}$$

Now our task is to estimate the term A_2. To do this task, we begin with the first part of this term by using the approximation properties of the interpolation operator and polynomial representative (cf. Lemma 3.1) in the following way

$$\begin{aligned}\sum_{K\in\mathcal{T}_h}a^K_{h,\mathrm{sym}}(\mathcal{I}\widehat{\boldsymbol{u}}-\widehat{\boldsymbol{u}}_\pi,\boldsymbol{\delta}_h)&\leq\sum_{K\in\mathcal{T}_h}a^K_{h,\mathrm{sym}}(\mathcal{I}\widehat{\boldsymbol{u}}-\widehat{\boldsymbol{u}},\boldsymbol{\delta}_h)+\sum_{K\in\mathcal{T}_h}a^K_{h,\mathrm{sym}}(\widehat{\boldsymbol{u}}-\widehat{\boldsymbol{u}}_\pi,\boldsymbol{\delta}_h)\\&\leq Ch^{\min\{s,k\}}|\widehat{\boldsymbol{u}}|_{1+s,\Omega}|\boldsymbol{\delta}_h|_{1,h}.\end{aligned}\tag{4.6}$$

Now for the second part of A_2, we invoke the polynomial approximation property given in Lemma 3.1 in order to obtain

$$\sum_{K\in\mathcal{T}_h}a^K_{h,\mathrm{sym}}(\widehat{\boldsymbol{u}}_\pi-\widehat{\boldsymbol{u}},\boldsymbol{\delta}_h)\leq Ch^{\min\{s,k\}}|\widehat{\boldsymbol{u}}|_{1+s,\Omega}|\boldsymbol{\delta}_h|_{1,h}.\tag{4.7}$$

Hence, gathering (4.6) and (4.7) we have $A_2\leq Ch^{\min\{s,k\}}|\widehat{\boldsymbol{u}}|_{1+s,\Omega}|\boldsymbol{\delta}_h|_{1,h}$. To bound A_3, we use the approximation properties of the projection operator $\mathbf{L}^2$ and, following the arguments of [36] we obtain

$$A_3=c(\boldsymbol{f},\boldsymbol{\delta}_h)-c_h(\boldsymbol{f},\boldsymbol{\delta}_h)\leq Ch^{\min\{s,k\}}|\boldsymbol{f}|_{s-1,\Omega}|\boldsymbol{\delta}_h|_{1,h}.\tag{4.8}$$

Now, we focus to bound the consistency error $\boldsymbol{\mathcal{N}}_h(\cdot,\cdot)$ as follows

$$\begin{aligned}(4.9)\quad \boldsymbol{\mathcal{N}}_h((\widehat{\boldsymbol{u}},\widehat{p}),\boldsymbol{\delta}_h) &:= \sum_{K\in\mathcal{T}_h} a^K(\widehat{\boldsymbol{u}},\boldsymbol{\delta}_h) + b_h(\boldsymbol{\delta}_h,\widehat{p}) - c(\boldsymbol{f},\boldsymbol{\delta}_h)\\ &= \sum_{e\in\mathcal{E}_{\text{int}}}\int_e \left(\nabla\widehat{\boldsymbol{u}} - \frac{1}{2}(\widehat{\boldsymbol{u}}\otimes\boldsymbol{\beta}) - \widehat{p}\mathbf{I}\right)\boldsymbol{n}_e\cdot[\![\boldsymbol{\delta}_h]\!],\end{aligned}$$

where $\mathbf{I}$ is identity matrix of size 2×2. For a better representation of the analysis, we define $\boldsymbol{\gamma} := \nabla\widehat{\boldsymbol{u}} - \frac{1}{2}(\boldsymbol{\beta}\otimes\widehat{\boldsymbol{u}})^T - \widehat{p}\mathbf{I}$. By employing orthogonality of the polynomial projection operator, we rewrite the term as follows

$$\begin{aligned}\boldsymbol{\mathcal{N}}_h((\widehat{\boldsymbol{u}},\widehat{p}),\delta_h) &= \sum_{e\in\mathcal{E}_{\text{int}}}\int_e(\boldsymbol{\gamma} - \boldsymbol{\Pi}^0_{k-1,K}\boldsymbol{\gamma})\boldsymbol{n}_e\cdot[\![\boldsymbol{\delta}_h - \boldsymbol{\mathcal{P}}_0\boldsymbol{\delta}_h]\!]\\ &\le \|\boldsymbol{\gamma} - \boldsymbol{\Pi}^0_{k-1,K}\boldsymbol{\gamma}\|_{e,0}\ \|\boldsymbol{\delta}_h - \boldsymbol{\mathcal{P}}_0\boldsymbol{\delta}_h\|_{e,0},\end{aligned}$$

where $\boldsymbol{\mathcal{P}}_0$ is the projection operator on constant polynomial space. By using trace inequality and approximation properties of the $\mathbf{L}^2$ projection operator, we derive as

$$(4.10)\qquad \|\boldsymbol{\gamma} - \boldsymbol{\Pi}^0_{k-1,K}\boldsymbol{\gamma}\|_{e,0} \le Ch^{\min\{s,k\}-\frac{1}{2}}|\boldsymbol{\gamma}|_{s,K}.$$

By using the approximation property of the $\mathbf{L}^2$ projection operator $\boldsymbol{\mathcal{P}}_0$, we derive the bound as follows:

$$(4.11)\qquad \|[\![\boldsymbol{\delta}_h]\!]\|_{0,e} \le Ch^{1/2}|\boldsymbol{\delta}_h|_{1,K}.$$

By employing inequalities (4.10), and (4.11), we bound the consistency error as follows

$$(4.12)\qquad \boldsymbol{\mathcal{N}}_h((\widehat{\boldsymbol{u}},\widehat{p}),\boldsymbol{\delta}_h) \le Ch^{\min\{s,k\}}\left(|\widehat{\boldsymbol{u}}|_{1+s,\Omega} + |\widehat{p}|_{s,\Omega}\right)|\boldsymbol{\delta}_h|_{1,h}.$$

Upon inserting estimates (4.5),(4.6), (4.7), (4.8), and (4.12) into (4.1), we obtain the bound

$$(4.13)\qquad \|\widehat{\boldsymbol{u}} - \widehat{\boldsymbol{u}}_h\|_{1,h} \le Ch^{\min\{s,k\}}\left(|\widehat{\boldsymbol{u}}|_{1+s,\Omega} + |\widehat{p}|_{s,\Omega} + |\boldsymbol{f}|_{s-1,\Omega}\right).$$

Further following the analogous arguments as [35, Theorem 13], and the bound of polynomial consistency error for the convective term, we derive the estimate for pressure variable, i.e.,

$$(4.14)\qquad \|\widehat{p} - \widehat{p}_h\|_{0,\Omega} \le Ch^{\min\{s,k\}}\left(|\widehat{\boldsymbol{u}}|_{1+s,\Omega} + |\widehat{p}|_{s,\Omega} + |\boldsymbol{f}|_{s-1,\Omega}\right).$$

Upon using (4.13) and (4.14) we obtain the desire result.

4.1. $\mathbf{L}^2$ Error estimates for the velocity.

In this part, we would like to bound the error in $\mathbf{L}^2$ norm. To achieve the goal, we first define the dual problem as follows: Find $(\boldsymbol{\psi},\xi)\in\mathcal{X}$ such that

$$\begin{aligned}(4.15)&\qquad -\nu\Delta\boldsymbol{\psi} - \operatorname{div}(\boldsymbol{\psi}\otimes\boldsymbol{\beta}) - \nabla\xi = (\widehat{\boldsymbol{u}} - \widehat{\boldsymbol{u}}_h)\quad \text{in } \Omega,\\ (4.16)&\qquad \operatorname{div}\boldsymbol{\psi} = 0\quad \text{in } \Omega,\\ (4.17)&\qquad (\xi,1) = 0\quad \text{in } \Omega,\\ (4.18)&\qquad \boldsymbol{\psi} = 0\quad \text{on } \partial\Omega.\end{aligned}$$

The model problem (4.15)-(4.18) is well posed. By applying the classical regularity theorem, we derive that

$$\|\boldsymbol{\psi}\|_{2,\Omega} + \|\xi\|_{1,\Omega} \leq \|\widehat{\boldsymbol{u}} - \widehat{\boldsymbol{u}}_h\|_{0,\Omega}. \tag{4.19}$$

By multiplying $\boldsymbol{v}_h = \widehat{\boldsymbol{u}} - \widehat{\boldsymbol{u}}_h$ in (4.15), we derive that

$$\int_\Omega \Big(-\nu\Delta\boldsymbol{\psi} - \operatorname{div}(\boldsymbol{\psi}\otimes\boldsymbol{\beta}) - \nabla\xi\Big)(\widehat{\boldsymbol{u}} - \widehat{\boldsymbol{u}}_h) = \|\widehat{\boldsymbol{u}} - \widehat{\boldsymbol{u}}_h\|^2_{0,\Omega}. \tag{4.20}$$

Now, since $\nabla\cdot\boldsymbol{\beta} = 0$, by employing integration by parts, we rewrite (4.20) as follows

$$\begin{aligned} \|\widehat{\boldsymbol{u}} - \widehat{\boldsymbol{u}}_h\|^2_{0,\Omega} &= \widehat{a}(\widehat{\boldsymbol{u}} - \widehat{\boldsymbol{u}}_h, \boldsymbol{\psi}) - b_h(\widehat{\boldsymbol{u}} - \widehat{\boldsymbol{u}}_h, \xi) \\ &\quad + \sum_{e\in\mathcal{E}} \int_e \left(-\nabla\boldsymbol{\psi} - \frac{1}{2}(\boldsymbol{\psi}\otimes\boldsymbol{\beta}) - \xi\mathbf{I}\right)\boldsymbol{n}_e \cdot [\![\widehat{\boldsymbol{u}} - \widehat{\boldsymbol{u}}_h]\!]. \end{aligned} \tag{4.21}$$

By employing the arguments as (4.12), and classical regularity result (4.19), we bound the following term as follows

$$\begin{aligned} \sum_{e\in\mathcal{E}} \int_e \left(-\nabla\boldsymbol{\psi} - \frac{1}{2}(\boldsymbol{\psi}\otimes\boldsymbol{\beta}) - \xi\mathbf{I}\right)\boldsymbol{n}_e \cdot [\![\widehat{\boldsymbol{u}} - \widehat{\boldsymbol{u}}_h]\!] &\leq Ch(|\boldsymbol{\psi}|_{2,\Omega} + |\xi|_{1,\Omega})\|\widehat{\boldsymbol{u}} - \widehat{\boldsymbol{u}}_h\|_{1,h} \\ &\leq Ch^{\min\{s,k\}+1}(|\widehat{\boldsymbol{u}}|_{1+s,\Omega} + |\widehat{p}|_{s,\Omega} + |\boldsymbol{f}|_{s-1,\Omega})\|\widehat{\boldsymbol{u}} - \widehat{\boldsymbol{u}}_h\|_{0,\Omega}. \end{aligned} \tag{4.22}$$

Further, using the fact that $b_h(\widehat{\boldsymbol{u}} - \widehat{\boldsymbol{u}}_h, \mathcal{R}_h\xi) = 0$, we rewrite the terms as follows

$$\begin{aligned} & a(\widehat{\boldsymbol{u}} - \widehat{\boldsymbol{u}}_h, \boldsymbol{\psi}) - b_h(\widehat{\boldsymbol{u}} - \widetilde{\boldsymbol{u}}_h, \xi) \\ &\quad = a(\widehat{\boldsymbol{u}} - \widehat{\boldsymbol{u}}_h, \boldsymbol{\psi} - \mathcal{I}\boldsymbol{\psi}) - b_h(\widehat{\boldsymbol{u}} - \widehat{\boldsymbol{u}}_h, \xi - \mathcal{R}_h\xi) + a(\widehat{\boldsymbol{u}} - \widehat{\boldsymbol{u}}_h, \mathcal{I}\boldsymbol{\psi}). \end{aligned} \tag{4.23}$$

By employing the estimate (4.13), approximation properties of the interpolation operator, and regularity result (Eqn (4.19)) we find

$$\begin{aligned} & a(\widehat{\boldsymbol{u}} - \widehat{\boldsymbol{u}}_h, \boldsymbol{\psi} - \mathcal{I}\boldsymbol{\psi}) - b_h(\widehat{\boldsymbol{u}} - \widehat{\boldsymbol{u}}_h, \xi - \mathcal{R}_h\xi) \\ &\quad \leq C\|\boldsymbol{\beta}\|_{\infty,\Omega}\|\widehat{\boldsymbol{u}} - \widehat{\boldsymbol{u}}_h\|_{1,h}\|\boldsymbol{\psi} - \mathcal{I}\boldsymbol{\psi}\|_{1,h} + \|\widehat{\boldsymbol{u}} - \widehat{\boldsymbol{u}}_h\|_{1,h}\|\xi - \mathcal{R}_h\xi\|_{0,\Omega} \\ &\quad \leq C\|\boldsymbol{\beta}\|_{\infty,\Omega}h^{\min\{s,k\}}(|\widehat{\boldsymbol{u}}|_{1+s,\Omega} + |\widehat{p}|_{s,\Omega} + |\boldsymbol{f}|_{s-1,\Omega})(|\boldsymbol{\psi}|_{2,\Omega} + \|\xi\|_{1,\Omega})h \\ &\quad\quad \leq C\|\boldsymbol{\beta}\|_{\infty,\Omega}h^{\min\{s,k\}+1}(|\widehat{\boldsymbol{u}}|_{1+s,\Omega} + |\widehat{p}|_{s,\Omega} + |\boldsymbol{f}|_{s-1,\Omega})\|\widehat{\boldsymbol{u}} - \widehat{\boldsymbol{u}}_h\|_{0,\Omega}. \end{aligned} \tag{4.24}$$

Further, with the estimate $b(\boldsymbol{\psi}, \widehat{p} - \widehat{p}_h) = 0$, we rewrite the last term of (4.23) as follows

$$\begin{aligned} a(\widehat{\boldsymbol{u}} - \widehat{\boldsymbol{u}}_h, \mathcal{I}\boldsymbol{\psi}) &= a(\widehat{\boldsymbol{u}}, \mathcal{I}\boldsymbol{\psi}) - a(\widehat{\boldsymbol{u}}_h, \mathcal{I}\boldsymbol{\psi}) \\ &= \Big(a(\widehat{\boldsymbol{u}}, \mathcal{I}\boldsymbol{\psi}) + b(\mathcal{I}\boldsymbol{\psi}, \widehat{p}) - c(\boldsymbol{f}, \mathcal{I}\boldsymbol{\psi})\Big) + \Big(a_h(\widehat{\boldsymbol{u}}_h, \mathcal{I}\boldsymbol{\psi}) - a(\widehat{\boldsymbol{u}}_h, \mathcal{I}\boldsymbol{\psi})\Big) \\ &\quad + \Big(c(\boldsymbol{f}, \mathcal{I}\boldsymbol{\psi}) - c_h(\boldsymbol{f}, \mathcal{I}\boldsymbol{\psi})\Big) + b(\boldsymbol{\psi} - \mathcal{I}\boldsymbol{\psi}, \widehat{p} - \widehat{p}_h). \end{aligned} \tag{4.25}$$

Since $\mathcal{I}\boldsymbol{\psi} \in \boldsymbol{\mathcal{U}}_h$, the term $a(\widehat{\boldsymbol{u}}, \mathcal{I}\boldsymbol{\psi}) + b(\mathcal{I}\boldsymbol{\psi}, \widehat{p}) - c(\boldsymbol{f}, \mathcal{I}\boldsymbol{\psi})$ measures the inconsistency due to non-conforming property of the discrete space. By using analogous arguments as (4.9), we bound the term

$$a(\widehat{\boldsymbol{u}}, \mathcal{I}\boldsymbol{\psi}) + b(\mathcal{I}\boldsymbol{\psi}, \widehat{p}) - c(\boldsymbol{f}, \mathcal{I}\boldsymbol{\psi}) \leq Ch^{\min\{s,k\}+1}(|\widehat{\boldsymbol{u}}|_{1+s,\Omega} + |\widehat{p}|_{s,\Omega})\|\widehat{\boldsymbol{u}} - \widehat{\boldsymbol{u}}_h\|_{0,\Omega}. \tag{4.26}$$

Upon employing the boundedness of the $\mathbf{L}^2$ projection operator, result (4.19), we bound the discrete load term as follows

$$c(\boldsymbol{f}, \mathcal{I}\boldsymbol{\psi}) - c_h(\boldsymbol{f}, \mathcal{I}\boldsymbol{\psi}) \leq Ch^{\min\{s,k\}+1}|\boldsymbol{f}|_{s-1,\Omega}\|\widehat{\boldsymbol{u}} - \widehat{\boldsymbol{u}}_h\|_{0,\Omega}. \tag{4.27}$$

Using the approximation properties of the interpolation operator and estimate (4.13), we derive that

$$b(\boldsymbol{\psi} - \mathcal{I}\boldsymbol{\psi}, \widehat{p} - \widehat{p}_h) \leq Ch^{\min\{s,k\}+1}|\widehat{\boldsymbol{u}}|_{1+s,\Omega}\|\widehat{\boldsymbol{u}} - \widehat{\boldsymbol{u}}_h\|_{0,\Omega}. \tag{4.28}$$

Now, we focus to bound the term $(a_h(\widehat{\boldsymbol{u}}_h, \mathcal{I}\boldsymbol{\psi}) - a(\widehat{\boldsymbol{u}}_h, \mathcal{I}\boldsymbol{\psi}))$ as follows

$$\begin{aligned} a_h(\widehat{\boldsymbol{u}}_h, \mathcal{I}\boldsymbol{\psi}) - a(\widehat{\boldsymbol{u}}_h, \mathcal{I}\boldsymbol{\psi}) = \sum_{K\in\mathcal{T}_h} \Big[& a_h^K(\widehat{\boldsymbol{u}}_h - \boldsymbol{\Pi}_K^0\widehat{\boldsymbol{u}}, \mathcal{I}\boldsymbol{\psi} - \boldsymbol{\Pi}_{1,K}^0\boldsymbol{\psi}) \\ & - a^K(\widehat{\boldsymbol{u}}_h - \boldsymbol{\Pi}_K^0\widehat{\boldsymbol{u}}, \mathcal{I}\boldsymbol{\psi} - \boldsymbol{\Pi}_{1,K}^0\boldsymbol{\psi}) + a_h^K(\boldsymbol{\Pi}_K^0\widehat{\boldsymbol{u}}, \mathcal{I}\boldsymbol{\psi}) - a^K(\boldsymbol{\Pi}_K^0\widehat{\boldsymbol{u}}, \mathcal{I}\boldsymbol{\psi}) \\ & + a_h^K(\widehat{\boldsymbol{u}}_h, \boldsymbol{\Pi}_{1,K}^0\boldsymbol{\psi}) - a^K(\widehat{\boldsymbol{u}}_h, \boldsymbol{\Pi}_{1,K}^0\boldsymbol{\psi})\Big]. \end{aligned} \tag{4.29}$$

By using the approximation properties of the projection operator and interpolation operator, we bound the term as follows

$$\sum_{K\in\mathcal{T}_h} a_h^K(\widehat{\boldsymbol{u}}_h, \mathcal{I}\boldsymbol{\psi}) - a^K(\widehat{\boldsymbol{u}}_h, \mathcal{I}\boldsymbol{\psi}) \leq Ch^{\min\{s,k\}+1}|\widehat{\boldsymbol{u}}|_{1+s,\Omega}\|\widehat{\boldsymbol{u}} - \widehat{\boldsymbol{u}}_h\|_{0,\Omega}. \tag{4.30}$$

By inserting the estimates (4.26), (4.27),(4.28), (4.29), (4.30) into (4.25), we obtain

$$a(\widehat{\boldsymbol{u}} - \widehat{\boldsymbol{u}}_h, \mathcal{I}\psi) \leq Ch^{\min\{s,k\}+1}|\widehat{\boldsymbol{u}}|_{1+s,\Omega}\|\widehat{\boldsymbol{u}} - \widehat{\boldsymbol{u}}_h\|_{0,\Omega}. \tag{4.31}$$

Using the estimates (4.22), (4.24), and (4.31) into (4.21), we derive

$$\|\widehat{\boldsymbol{u}} - \widehat{\boldsymbol{u}}_h\|_{0,\Omega} \leq Ch^{\min\{s,k\}+1}(|\widehat{\boldsymbol{u}}|_{1+s,\Omega} + |\widehat{p}|_{s,\Omega} + |\boldsymbol{f}|_{s-1,\Omega}).$$

□

We have the following consequence

Lemma 4.2. *There exists a constant $C > 0$ independent of mesh size h such that*

$$\|(\boldsymbol{T} - \boldsymbol{T}_h)\boldsymbol{f}\|_{0,\Omega} \leq Ch^{\min\{s,k\}+1}(|\widehat{\boldsymbol{u}}|_{1+s,\Omega} + |\widehat{p}|_{s,\Omega} + |\boldsymbol{f}|_{s-1,\Omega}).$$

The above statement is state forward due to previous result, and Theorem 2.1. The next results establish the convergence of the operator $\boldsymbol{T}_h^*$ to $\boldsymbol{T}^*$ as h goes to zero in broken norm and in the $\mathbf{L}^2$ norm. The proof can be obtained repeating the same arguments as those used in the previous section.

Theorem 4.3. *Let $\boldsymbol{f} \in \mathbf{L}^2(\Omega, \mathbb{C}) \cap \mathbf{H}^{s^*-1}(\Omega)$ be such that $\widehat{\boldsymbol{u}}^* := \boldsymbol{T}^*\boldsymbol{f}$ and $\widehat{\boldsymbol{u}}_h^* := \boldsymbol{T}_h^*\boldsymbol{f}$. Then, there exists a positive constant C, independent of h, such that*

$$\|(\boldsymbol{T}^* - \boldsymbol{T}_h^*)\boldsymbol{f}\|_{1,h} = \|\widehat{\boldsymbol{u}}^* - \widehat{\boldsymbol{u}}_h^*\|_{1,h} \leq Ch^{\min\{k,s^*\}}\Big(|\widehat{\boldsymbol{u}}^*|_{1+s^*,\Omega} + |\widehat{p}^*|_{s^*,\Omega} + \|\boldsymbol{f}\|_{s^*-1,\Omega}\Big).$$

$$\|(\boldsymbol{T}^* - \boldsymbol{T}_h^*)\boldsymbol{f}\|_{0,\Omega} = \|\widehat{\boldsymbol{u}}^* - \widehat{\boldsymbol{u}}_h^*\|_{0,\Omega} \leq Ch^{\min\{k,s^*\}+1}\Big(|\widehat{\boldsymbol{u}}^*|_{1+s^*,\Omega} + |\widehat{p}^*|_{s^*,\Omega} + \|\boldsymbol{f}\|_{s^*-1,\Omega}\Big).$$

where C is a positive constant independent of h.

As a consequence of the previous results is that, according to the theory of [21], we are in a position to conclude that our numerical method does not introduce spurious eigenvalues. This is stated in the following theorem.

THEOREM 4.4. *Let $V \subset \mathbb{C}$ be an open set containing $\operatorname{sp}(\boldsymbol{T})$. Then, there exists $h_0 > 0$ such that $\operatorname{sp}(\boldsymbol{T}_h) \subset V$ for all $h < h_0$.*

5. Spectral approximation and error estimates:. We will obtain convergence and error estimates for the suggested nonconforming VEM discretization for the Oseen eigenvalue problem in this section. More precisely, we shall prove that $\boldsymbol{T}_h$ gives a valid spectral approximation of $\boldsymbol{T}$ by using the classical theory for compact operators (see [10]). The equivalent adjoint operators $\boldsymbol{T}_h^*$ and $\boldsymbol{T}^*$ of $\boldsymbol{T}_h$ and $\boldsymbol{T}$, respectively, will then have a comparable convergence result established. First, let's review what spectral projectors are. Let μ be an algebraic multiplicity m nonzero eigenvalue of $\boldsymbol{T}$. C sets a circle with a centre at μ in the complex plane, ensuring that no other eigenvalue is contained inside C. Furthermore, think about the spectral projections E and E^* in the manner described below:

$$E := (2\pi i)^{-1}\int_C (z - \boldsymbol{T})^{-1}dz \qquad E^* := (2\pi i)^{-1}\int_C (z - \boldsymbol{T}^*)^{-1}dz,$$

where E and E^* are projections onto the space of generalized eigenvectors $R(E)$ and $R(E^*)$, respectively. Now, it is easy to prove that $R(E), R(E^*) \in \mathbf{H}^{r+1} \times \mathbf{H}^r$, and $R(E^*) \in \mathbf{H}^{r^*+1} \times \mathbf{H}^{r^*}$(see Theorem 2.1 and 2.3). Next, since $\boldsymbol{T}_h$ converges to $\boldsymbol{T}$, it means that there exist m eigenvalues (which lie in C) $\mu(1), \ldots, \mu(m)$ of $\boldsymbol{T}_h$ (repeated according to their respective multiplicities) which will converge to μ as h goes to zero. In the same sense, we introduce the following spectral projector $E_h := (2\pi i)^{-1}\int_C (z-\boldsymbol{T}_h)^{-1}dz$, which is a projector onto the invariant subspace $R(E_h)$ of $\boldsymbol{T}_h$ spanned by the generalized eigenvectors of $\boldsymbol{T}_h$ corresponding to $\mu(1), \ldots, \mu(m)$. We also recall the definition of gap $\widehat{\delta}$ between the closed subspaces $\boldsymbol{\mathcal{X}}$, and $\boldsymbol{\mathcal{Y}}$ of $\mathbf{L}^2$.

$$\widehat{\delta}(\boldsymbol{\mathcal{X}}, \boldsymbol{\mathcal{Y}}) := \max\{\delta(\boldsymbol{\mathcal{X}}, \boldsymbol{\mathcal{Y}}), \delta(\boldsymbol{\mathcal{Y}}, \boldsymbol{\mathcal{X}})\},$$

where

$$\delta(\boldsymbol{\mathcal{X}}, \boldsymbol{\mathcal{Y}}) = \sup_{\mathbf{x}\in\boldsymbol{\mathcal{X}};\|\mathbf{x}\|_{\mathbf{L}^2}=1} \delta(\mathbf{x}, \boldsymbol{\mathcal{Y}}), \quad \text{with } \delta(\boldsymbol{x}, \boldsymbol{\mathcal{Y}}) = \inf_{\mathbf{y}\in\boldsymbol{\mathcal{Y}};\|\mathbf{y}\|_{\mathbf{L}^2}=1} \|\mathbf{x} - \mathbf{y}\|_{\mathbf{L}^2}.$$

The following error estimates for the approximation of eigenvalues and eigenfunctions hold true.

THEOREM 5.1. *There exists a strictly positive constant C such that*

$$\widehat{\delta}(R(E), R(E_h)) \leq Ch^{\min\{r,k\}+1}; \tag{5.1}$$

$$|\mu - \widehat{\mu}_h| \leq Ch^{\min\{r,k\}+\min\{r^*,k\}}, \tag{5.2}$$

where $\widehat{\mu}_h := \frac{1}{m}\sum_{j=1}^m \mu_h^j$, where $r \geq 1$, and $r^* \geq 1$ are the orders of regularity of the eigenfunctions of primal and dual problems.

Proof. The estimate (5.1) follows from [10, Theorem 7.1], and the fact that $\|\boldsymbol{T}_h - \boldsymbol{T}\|_{0,\Omega} \approx O(h^{\min\{r,k\}+1})$ (Lemma 4.2). In what follows we will prove (5.2): assume that $\boldsymbol{T}(\boldsymbol{u}_j) = \mu \boldsymbol{u}_j$, for $j = 1, 2, \ldots, m$. Since $A(\cdot,\cdot)$ is an inner-product, we can choose a dual basis for $R(E^*)$ denoted by $(\boldsymbol{u}_j^*)$ satisfying

$$\langle \boldsymbol{u}_j, \boldsymbol{u}_l^* \rangle := A(\boldsymbol{u}_j, \boldsymbol{u}_l^*) = \delta_{jl}, \tag{5.3}$$

where $\langle \cdot,\cdot\rangle$ denotes the corresponding duality pairing. Now, from [10, Theorem 7.2], we have that

$$|\mu - \widehat{\mu}_h| \leq \frac{1}{m}\sum_{k=1}^{m} \Big|\langle (\boldsymbol{T} - \boldsymbol{T}_h)\boldsymbol{u}_k, \boldsymbol{u}_k^* \rangle\Big| + \|(\boldsymbol{T} - \boldsymbol{T}_h)|_{R(E)}\|_{0,\Omega} \|(\boldsymbol{T}^* - \boldsymbol{T}_h^*)|_{R(E)}\|_{0,\Omega}, \tag{5.4}$$

where $\langle \cdot,\cdot\rangle$ denotes the corresponding duality pairing. The estimate of the second term of (5.4) is quite obvious. In this direction, we need bound of $\|(\boldsymbol{T} - \boldsymbol{T}_h)\|_{0,\Omega}$, and $\|(\boldsymbol{T}^* - \boldsymbol{T}_h^*)\|_{0,\Omega}$ which are achieved from Lemma 4.2, and Theorem 4.3. However, the estimate of $\langle (\boldsymbol{T} - \boldsymbol{T}_h)\boldsymbol{u}_k, \boldsymbol{u}_k^*\rangle$ is not straightforward, and it needs arguments same as [4].

$$\begin{aligned}
\langle (\boldsymbol{T} - \boldsymbol{T}_h)\boldsymbol{u}_k, \boldsymbol{u}_k^*\rangle &= A((\boldsymbol{T} - \boldsymbol{T}_h)\boldsymbol{u}_k, p_k - p_{k,h}); (\boldsymbol{u}_k^*, p_k^*)) \\
&= A((\boldsymbol{T} - \boldsymbol{T}_h)\boldsymbol{u}_k, p_k - p_{k,h}); (\boldsymbol{u}_k^*, p_k^*) - (\boldsymbol{v}_h, \eta_h)) \\
&\quad + A((\boldsymbol{T}\boldsymbol{u}_k, p_k); (\boldsymbol{v}_h, \eta_h)) - A((\boldsymbol{T}_h\boldsymbol{u}_k, p_{k,h}); (\boldsymbol{v}_h, \eta_h)) \\
&= A((\boldsymbol{T} - \boldsymbol{T}_h)\boldsymbol{u}_k, p_k - p_{k,h}); (\boldsymbol{u}_k^*, p_k^*) - (\boldsymbol{v}_h, \eta_h)) + c(\boldsymbol{u}_k, \boldsymbol{v}_h) \\
&+ \boldsymbol{\mathcal{N}}_h((\boldsymbol{T}\boldsymbol{u}_k, p_k), \boldsymbol{v}_h) - A((\boldsymbol{T}_h u_k, p_{k,h}), (\boldsymbol{v}_h, \eta_h)) \\
&+ A_h((\boldsymbol{T}_h u_k, p_{k,h}), (\boldsymbol{v}_h, \eta_h)) - c_h(\boldsymbol{u}_k, \boldsymbol{v}_h).
\end{aligned} \tag{5.5}$$

In the above estimate, the consistency error $\boldsymbol{\mathcal{N}}_h(\cdot,\cdot)$ appears since $\boldsymbol{\mathcal{U}}_h \not\subset \mathbf{H}^1(\Omega)$. Now, we proceed to bound the terms appeared in (5.5). In (5.5), we have mentioned that $(\boldsymbol{v}_h, \eta_h) \in \boldsymbol{\mathcal{U}}_h \times \mathrm{Q}_h$ is any discrete function. However, to achieve optimal rate of convergence of the spectrum, choose $(\boldsymbol{v}_h, \eta_h) := (\mathcal{I}\boldsymbol{u}_k^*, \mathcal{R}_h p_k^*)$. Upon employing, the approximation properties of the interpolation operator, we bound the term as follows:

$$\begin{aligned}
&A((\boldsymbol{T} - \boldsymbol{T}_h)\boldsymbol{u}_k, p_k - p_{k,h}), (\boldsymbol{u}_k^*, p_k^*) - (\mathcal{I}\boldsymbol{u}_k^*, \mathcal{R}_h p_k^*)) \\
&\quad \leq C\|(\boldsymbol{T} - \boldsymbol{T}_h)\boldsymbol{u}_k\|_{1,h}\|\boldsymbol{u}_k^* - \mathcal{I}\boldsymbol{u}_k^*\|_{1,h} + \|(\boldsymbol{T} - \boldsymbol{T}_h)\boldsymbol{u}_k\|_{1,h}\|p_k^* - \mathcal{R}_h p_k^*\|_{0,\Omega} \\
&\qquad + \|p_k - p_{k,h}\|_{0,\Omega}\|\boldsymbol{u}_k^* - \mathcal{I}\boldsymbol{u}_k^*\|_{1,h}.
\end{aligned} \tag{5.6}$$

By employing Lemma 3.1, and spectral convergence of the primal problem, we have

$$\begin{aligned}
&A((\boldsymbol{T} - \boldsymbol{T}_h)\boldsymbol{u}_k, p_k - p_{k,h}), (\boldsymbol{u}_k^*, p_k^*) - (\mathcal{I}\boldsymbol{u}_k^*, \mathcal{R}_h p_k^*)) \\
&\quad \leq Ch^{\min\{r,k\}+\min\{r^*,k\}}\Big(|\boldsymbol{u}_k|_{1+r,\Omega} + |p_k|_{r,\Omega} + |\boldsymbol{f}|_{r-1,\Omega}\Big)\Big(|\boldsymbol{u}_k^*|_{1+r^*,\Omega} + |p_k^*|_{r^*,\Omega}\Big).
\end{aligned} \tag{5.7}$$

By employing the polynomial consistency property of the load term and approximation property of the $\mathbf{L}^2$ projection operator, we have

$$\begin{aligned}
c(\boldsymbol{u}_k, \boldsymbol{v}_h) - c_h(\boldsymbol{u}_k, \boldsymbol{v}_h) = \sum_{K\in\mathcal{T}_h} & c^K(\boldsymbol{u}_k - \boldsymbol{u}_{k,\pi}, \mathcal{I}\boldsymbol{u}_k - \boldsymbol{u}_{k,\pi}) \\
& + c_h^K(\boldsymbol{u}_k - \boldsymbol{u}_{k,\pi}, \mathcal{I}\boldsymbol{u}_k - \boldsymbol{u}_{k,\pi}) \leq Ch^{2\min\{r,k\}+2}|\boldsymbol{u}_k|_{1+r,\Omega}.
\end{aligned} \tag{5.8}$$

The difference between continuous and discrete forms can be bounded as follows[4]

(5.9)
$$A_h((\boldsymbol{T}_h\boldsymbol{u}_k,p_{k,h}),(\mathcal{I}\boldsymbol{u}_k^*,\mathcal{R}_hp_k^*))-A((\boldsymbol{T}_h\boldsymbol{u}_k,p_{k,h}),(\mathcal{I}\boldsymbol{u}_k^*,\mathcal{R}_hp_k^*))$$
$$\leq Ch^{\min\{r,k\}+\min\{r^*,k\}}\Big(|\boldsymbol{u}_k|_{1+r,\Omega}+|p_k|_{r,\Omega}+|\boldsymbol{f}|_{r-1,\Omega}\Big)\Big(|\boldsymbol{u}_k^*|_{1+r^*,\Omega}+|p_k^*|_{r^*,\Omega}\Big).$$

In the above estimate, we have added and subtracted $\boldsymbol{\Pi}_K^0\boldsymbol{T}_h\boldsymbol{u}_k$, and applied the approximation properties of the interpolation operator. Now, we are in a situation to bound the variational crime associated with the formulation. Recollecting $\boldsymbol{\mathcal{N}}_h((\mu\boldsymbol{u}_k,p_k),\boldsymbol{u}_k^*)=0$, we rewrite the term as follows:

(5.10)
$$\begin{aligned}\boldsymbol{\mathcal{N}}_h((\mu\boldsymbol{u}_k,p_k),\mathcal{I}\boldsymbol{u}_k^*)&=\boldsymbol{\mathcal{N}}_h((\mu\boldsymbol{u}_k,p_k),\mathcal{I}\boldsymbol{u}_k^*-\boldsymbol{u}_k^*)\\&\leq Ch^{\min\{r,k\}}\Big(|\boldsymbol{u}_k|_{1+r,\Omega}+|p_k|_{r,\Omega}\Big)\Big(|\mathcal{I}\boldsymbol{u}_k^*-\boldsymbol{u}_k^*|_{1,h}\Big)\\&\leq Ch^{\min\{r,k\}+\min\{r^*,k\}}\Big(|\boldsymbol{u}_k|_{1+r,\Omega}+|p_k|_{r,\Omega}\Big)|\boldsymbol{u}_k^*|_{1+r^*,\Omega}.\end{aligned}$$

Upon inserting (5.7), (5.8), (5.9), and (5.10) into (5.5), we obtain an estimate for the term $\langle(\boldsymbol{T}-\boldsymbol{T}_h)\boldsymbol{u}_k,\boldsymbol{u}_k^*\rangle$, and consequently double order convergence of the spectrum, i.e., (5.4). ∎

6. Numerical experiments.

We end our paper reporting some numerical tests to illustrate the performance of our method. The implementation of the method has been developed in a Matlab code. The goal is to assess the performance of the method on different domains and of course, study the presence of spurious eigenvalues. After computing the eigenvalues, the rates of convergence are calculated by using a least-square fitting. More precisely, if λ_h is a discrete complex eigenvalue, then the rate of convergence α is calculated by extrapolation with the least square fitting

$$\lambda_h\approx\lambda_{\text{extr}}+Ch^{\alpha}, \tag{6.1}$$

where λ_{extr} is the extrapolated eigenvalue given by the fitting.

For the tests we consider the following families of polygonal meshes which satisfy the assumptions **A1** and **A2** (see Figure 1):

- $\mathcal{T}_h^1$: trapezoidal meshes;
- $\mathcal{T}_h^2$: squares meshes;
- $\mathcal{T}_h^3$: structured hexagonal meshes made of convex hexagons;
- $\mathcal{T}_h^4$: non-structured Voronoi meshes.

6.1. Test 1: a square domain.

In this first test, we have taken $\Omega=(-1,1)^2$, $\boldsymbol{\beta}=(1,0)^{\texttt{t}}$. On this type of domain, the eigenfunctions are sufficiently smooth due the convexity of the square and the null boundary conditions. Hence, an optimal order of convergence is expected with our method. For this test we consider the meshes reported in Figure 1. The results are contained in Table 1 where in the column "Order" we report the computed order of convergence for the eigenvalues, which has been obtained with the least square fitting (6.1), together with extrapolated values that we report on the column "Extr."

6.2. Test case 2: L shaped domain.

In this example, we consider non-convex domain which is called as L shaped domain, defined as $\Omega_L:=(-1,1)\times(-1,1)\setminus[-1,0]\times[-1,0]$(Figure 3). The eigenfunctions have singularity at $(0,0)$ therefore the convergence order of the corresponding eigenvalues are not optimal. According to

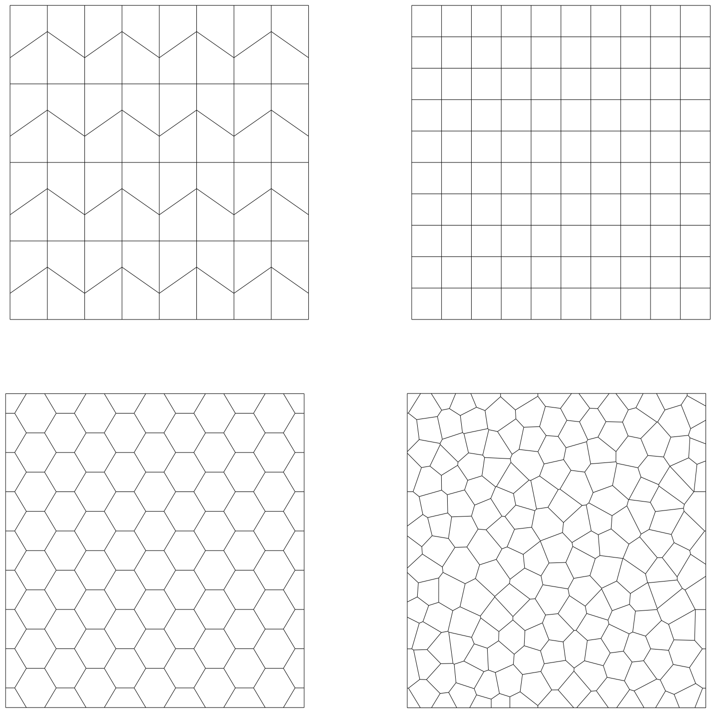

FIG. 1. *Sample meshes:* $\mathcal{T}_h^1$ *(top left),* $\mathcal{T}_h^2$ *(top right),* $\mathcal{T}_h^3$ *(bottom left),* $\mathcal{T}_h^4$ *(bottom right) for* $N = 8$ *and 10.*

the regularity of the eigenfunctions, the rate of convergence r for the eigenvalues is such that $1.7 \leq r \leq 2$. In Table 2, we display the results for the model problem. In Figures 4, we have dissected the first three discrete velocity and pressure fields. Table 2's results demonstrate that the approach provides the anticipated convergence behavior in the eigenvalue approximation. Because of the geometrical singularity of the re-entrant angle, the eigenfunction associated with the first eigenvalue is not sufficiently smooth when compared to the eigenfunctions of the other eigenvalues. The order of convergence for the first computed eigenvalue reflects this fact.

6.3. Spurious analysis. The aim of this test is to analyze numerically the influence of the stabilization parameter on the computation of the spectrum. It is well know that if this parameter is not correctly chosen, may appear spurious eigenvalues. We refer to [25, 23, 24, 31] where the VEM reports this phenomenon. It is well known that under some configurations of the domain, more precisely, convexity and boundary conditions, the arise of spurious eigenvalues when stabilized methods are considered compared when the same methods are implemented in domains with null boundary Dirichlet conditions. We refer to the reader to [25, 22] where this is discussed. Hence, for this experiment we consider the following problem: Given a domain $\Omega \subset \mathbb{R}^2$, let

TABLE 1
The lowest computed eigenvalues $\lambda_{h,i}$, $1 \leq i \leq 4$ on different meshes.

$\mathcal{T}_h$	$\lambda_{h,i}$	$N=16$	$N=32$	$N=64$	$N=128$	Order	Extr.	[27]
$\mathcal{T}_h^1$	$\lambda_{1,h}$	13.5455	13.5931	13.6054	13.6085	1.95	13.6097	13.6096
	$\lambda_{2,h}$	22.9603	23.0917	23.1204	23.1274	2.17	23.1291	23.1297
	$\lambda_{3,h}$	23.2729	23.3893	23.4147	23.4209	2.17	23.4223	23.4230
	$\lambda_{4,h}$	31.7714	32.1695	32.2658	32.2900	2.04	32.2973	32.2981
$\mathcal{T}_h^2$	$\lambda_{h,1}$	13.5670	13.5990	13.6069	13.6089	2.00	13.6096	13.6096
	$\lambda_{h,2}$	22.9501	23.0917	23.1206	23.1275	2.26	23.1289	23.1297
	$\lambda_{h,3}$	23.2825	23.3948	23.4163	23.4213	2.35	23.4221	234230
	$\lambda_{h,4}$	31.8671	32.1979	32.2735	32.2920	2.11	32.2971	32.2981
$\mathcal{T}_h^3$	$\lambda_{h,1}$	13.6980	13.6318	13.6151	13.6110	1.99	13.6095	13.6096
	$\lambda_{h,2}$	23.3644	23.1976	23.1472	23.1341	1.77	23.1277	23.1297
	$\lambda_{h,3}$	23.7112	23.4960	23.4411	23.4275	1.98	23.4227	23.4230
	$\lambda_{h,4}$	32.8415	32.4460	32.3354	32.3074	1.86	32.2951	32.2981
$\mathcal{T}_h^4$	$\lambda_{h,1}$	13.6935	13.6276	13.6135	13.6106	2.23	13.6097	13.6096
	$\lambda_{h,2}$	23.3782	23.1945	23.1443	23.1334	1.92	23.1280	23.1297
	$\lambda_{h,3}$	23.6837	23.4885	23.4379	23.4268	1.98	23.4219	23.4230
	$\lambda_{h,4}$	32.7775	32.4220	32.3255	32.3051	1.94	32.2951	32.2981

TABLE 2
The lowest computed eigenvalues $\lambda_{h,i}$, $1 \leq i \leq 4$ on different meshes.

$\mathcal{T}_h$	$\lambda_{h,i}$	$N=16$	$N=32$	$N=64$	$N=128$	Order	Extr.	[27]
$\mathcal{T}_h^5$	$\lambda_{1,h}$	31.6764	32.5080	32.8513	32.8855	1.65	32.8949	33.0306
	$\lambda_{2,h}$	36.6099	36.9845	37.0997	37.1058	2.02	37.1073	37.1106
	$\lambda_{3,h}$	41.8939	42.2468	42.3768	42.3878	1.79	42.3901	42.4023
	$\lambda_{4,h}$	48.7401	49.1200	49.2219	49.2247	2.19	49.2264	49.2552
$\mathcal{T}_h^6$	$\lambda_{h,1}$	31.2535	32.3647	32.7931	32.8151	1.76	32.8303	33.0306
	$\lambda_{h,2}$	36.1669	36.8918	37.0938	37.1058	2.13	37.1066	37.1106
	$\lambda_{h,3}$	41.8756	42.2558	42.3880	42.3978	1.86	42.4000	42.4023
	$\lambda_{h,4}$	49.4014	49.2980	49.2609	49.2577	1.82	49.2572	49.2552

us assume that its boundary $\partial\Omega$ is such that $\partial\Omega := \Gamma_D \cup \Gamma_N$ where $|\Gamma_D| > 0$.

$$\left\{\begin{array}{rcll} -\nu\Delta\boldsymbol{u} + (\boldsymbol{\beta}\cdot\nabla)\boldsymbol{u} + \nabla p & = & \lambda\boldsymbol{u} & \text{in}\,\Omega, \\ \operatorname{div}\boldsymbol{u} & = & 0 & \text{in}\,\Omega, \\ \boldsymbol{u} & = & \boldsymbol{0} & \text{on}\,\Gamma_D, \\ (\nu\nabla\boldsymbol{u} - p\boldsymbol{I})\cdot\boldsymbol{n} & = & \boldsymbol{0} & \text{on}\,\Gamma_N, \end{array}\right. \tag{6.2}$$

where $\boldsymbol{I} \in \mathbb{C}^{d\times d}$ is the identity matrix. Clearly from (6.2) a part of the boundary $\partial\Omega$ changes from Dirichlet to Neumann leading to a different configuration from problem(2.1) and hence, the stabilization term may introduce spuious eigenvalues that cannot being observed on a clamped domain. In particular, for the computational tests we have considered $\Omega := (0,1)^2$ and $\boldsymbol{\beta} := (1,0)^{\mathtt{t}}$ as convective term.

In Tables 3 and 4 we report the computed results for quadrilateral and voronoi meshes, respectively. From Table 3 we observe that when the stabilization parameter α_E is small, more precisely, is such that $\alpha_E < 1$, an important amount of spurious eigenvalues arise on the computed spectrum which start to vanish when α_E increases. This phenomenon is clear for both families of meshes $\mathcal{T}_h^1$ and $\mathcal{T}_h^2$. For other families

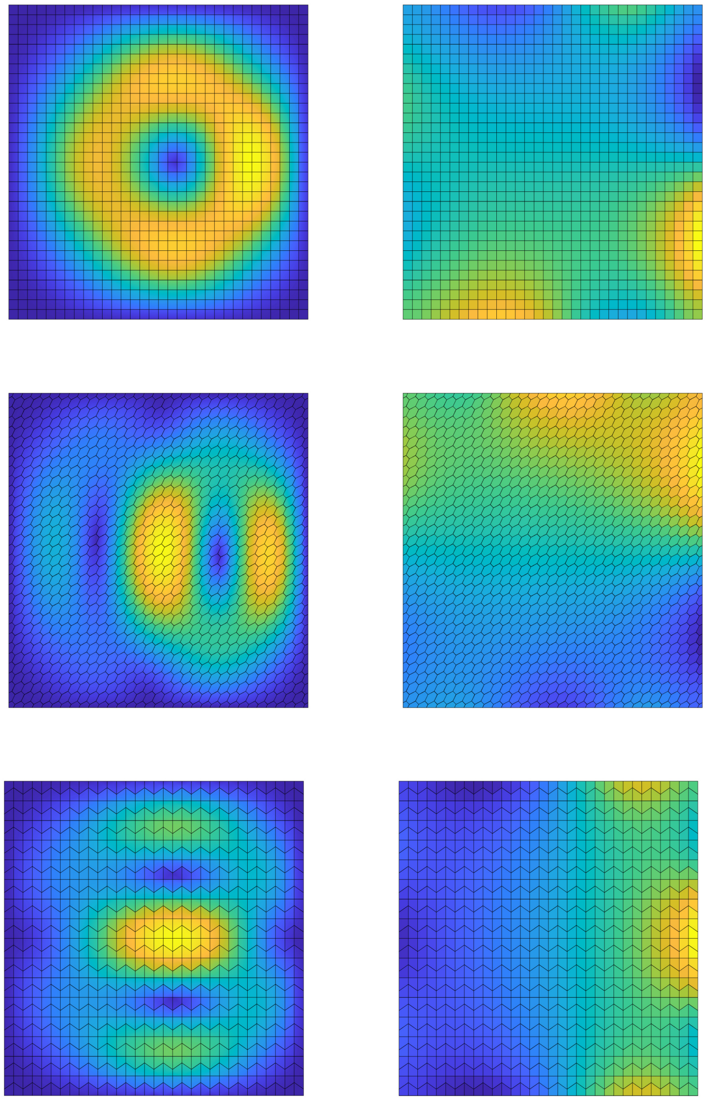

FIG. 2. *First, second and third magnitude of the eigenfunctions in the square together with the associated pressures: first column $u_{1,h}$, $u_{2,h}$ and $u_{3,h}$;second column: $p_{1,h}$, $p_{2,h}$ and $p_{3,h}$; for different family of meshes.*

695 of polygonal meshes the results are similar.

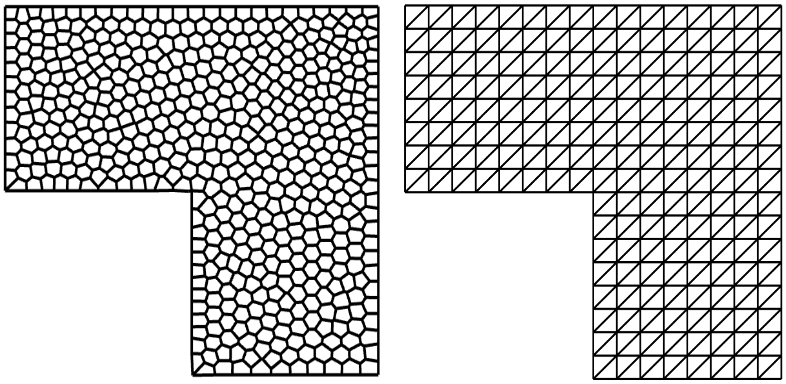

FIG. 3. *Sample meshes:* $\mathcal{T}_h^5$ *(left panel),* $\mathcal{T}_h^6$ *(right panel) for* $N = 8$

TABLE 3
Computed eigenvalues for different values of α_E *with* $\mathcal{T}_h^1$*.*

α_E=1/32	α_E=1/16	α_E=1/4	α_E=1	α_E=4	α_E=16	α_E=32
1.4756	2.0870	2.4106	2.4592	2.4699	2.4725	2.4729
1.6460	2.9541	5.0781	5.8418	6.1009	6.1942	6.2204
1.7314	3.4238	12.2493	14.9763	15.2397	15.3516	15.3869
1.7403	3.4620	12.9070	21.1375	22.3902	22.6216	22.6584
1.7434	3.4755	13.4713	24.3622	26.5618	27.0429	27.1458
1.7461	3.4866	13.5881	37.6233	43.4899	44.4647	44.6536
1.7465	3.4883	13.7754	40.5498	46.3123	47.5366	47.8232
1.7476	3.4931	13.8329	44.8864	62.6882	64.8430	65.1451
1.7476	3.4931	13.9038	45.6918	62.8106	65.2323	65.6622
1.7482	3.4954	13.9206	51.1740	73.0533	74.6701	75.0219

TABLE 4
Computed eigenvalues for different values of α_E *with* $\mathcal{T}_h^2$*.*

α_E=1/32	α_E=1/16	α_E=1/4	α_E=1	α_E=4	α_E=16	α_E=32
1.3079	1.9108	2.3682	2.4508	2.4693	2.4738	2.4746
1.4751	2.6176	4.7627	5.7418	6.1175	6.2326	6.2538
1.5773	3.1053	10.8813	14.9485	15.2728	15.3987	15.4251
1.5888	3.1537	11.6653	20.2761	22.3258	22.7300	22.7935
1.5929	3.1711	12.2935	23.3574	26.5470	27.1798	27.2809
1.5965	3.1857	12.5435	36.2960	43.3638	44.5662	44.7522
1.5970	3.1879	12.5978	38.9726	46.2787	47.8972	48.1768
1.5985	3.1940	12.6964	40.1479	61.8863	65.7328	66.2699
1.5986	3.1946	12.7105	41.7956	62.5039	66.1776	66.7132
1.5993	3.1973	12.7546	47.2934	73.3563	75.1252	75.4144

The natural question now is if the refinement of the meshes causes some behavior on the spurious eigenvalues. To observe this, in Table 5 we report the computed

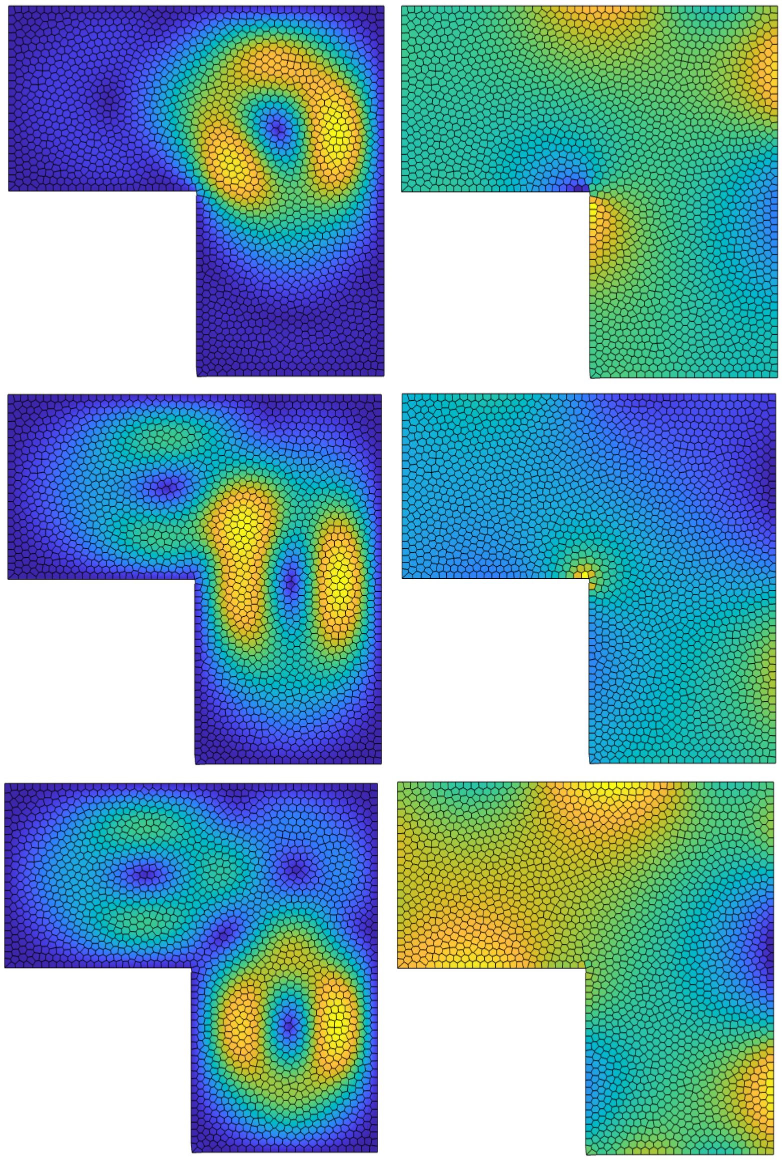

FIG. 4. *First, second and third magnitude of the eigenfunctions in the nonconvex L domain together with the associated pressures: first column $u_{1,h}$, $u_{2,h}$ and $u_{3,h}$;second column: $p_{1,h}$, $p_{2,h}$ and $p_{3,h}$; for different family of meshes.*

eigenvalues for $\alpha_E = 1/16$ and different refinements of the meshes $\mathcal{T}_h^1$ and $\mathcal{T}_h^2$.

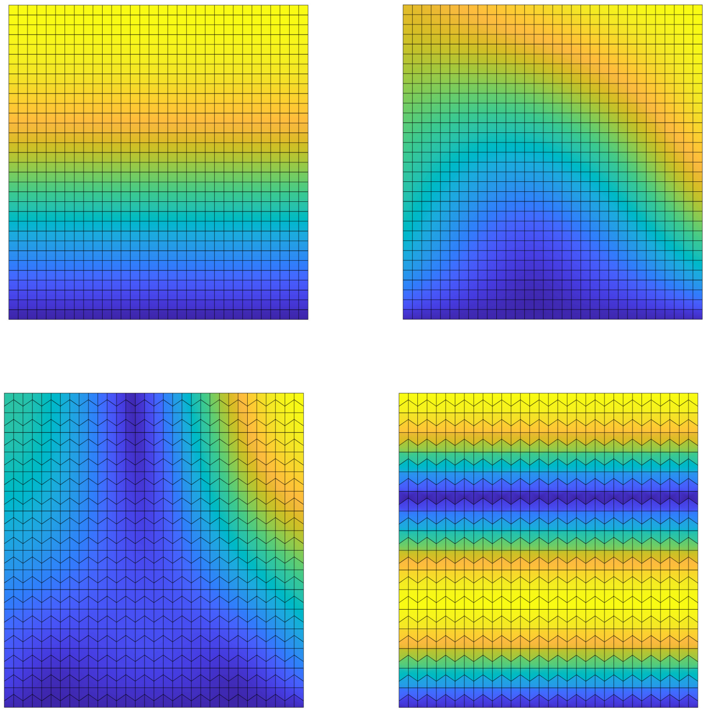

FIG. 5. *First, second and third magnitude of the eigenfunctions with $N = 32$, for different family of meshes.*

TABLE 5
First ten approximated eigenvalues for $\mathcal{T}_h^1$, $\mathcal{T}_h^2$ and $\alpha_E = 1/16$.

	$\mathcal{T}_h^1$				$\mathcal{T}_h^2$			
$\lambda_{i,h}$	$N = 8$	$N = 16$	$N = 32$	$N = 64$	$N = 8$	$N = 16$	$N = 32$	$N = 64$
$\lambda_{1,h}$	2.0870	2.4062	2.4536	2.4640	1.9108	2.3625	2.4434	2.4675
$\lambda_{2,h}$	2.9541	5.0980	5.9016	6.1662	2.6176	4.7627	5.7403	6.2711
$\lambda_{3,h}$	3.4238	12.1729	15.0548	15.3446	3.1053	10.7987	14.9670	15.4816
$\lambda_{4,h}$	3.4620	12.8841	20.7115	21.9155	3.1537	11.6268	19.7656	22.2157
$\lambda_{5,h}$	3.4755	13.5330	24.3679	26.5839	3.1711	12.2229	23.1339	27.1272
$\lambda_{6,h}$	3.4866	13.5547	36.9583	42.3002	3.1857	12.5104	35.4604	43.3846
$\lambda_{7,h}$	3.4883	13.7505	40.8357	46.9367	3.1879	12.5338	38.5668	48.4105
$\lambda_{8,h}$	3.4931	13.7849	43.3386	59.0853	3.1940	12.6514	38.8406	61.7552
$\lambda_{9,h}$	3.4931	13.8772	45.3771	61.8600	3.1946	12.6648	41.0988	64.6454
$\lambda_{10,h}$	3.4954	13.8772	50.2525	73.6216	3.1973	12.7087	45.7664	75.3587

Table 5 reveals that a refinement strategy is capable to avoid the spurious eigenvalues from the spectrum. This is an important fact that confirms the good properties fo the NCVEM on our eigenvalue context. In fact, we observe that when $\alpha_E = 1/16$ is considered, the spectrum gets cleaner when the mesh is refined. Moreover, this test suggests that $\alpha_E = 1$ is a suitable value to be considered for the approximation as in, for instance, [15].

7. Conclusion. For the nonsymmetric Oseen eigenvalue problem, we have presented a divergence-free, arbitrary-order accurate, nonconforming virtual element approach that applies to highly generic shaped polygonal domains. We performed a convergence study of the eigenfunctions using a solution operator on the continuous space. In addition, we utilized the idea of compact operators to define the discrete operator associated to the discrete problem and demonstrate the convergence of the approach. In the end, we were able to retrieve the double order of convergence of the eigenvalues by taking use of the extra regularity of the eigenfunctions. Our next area of interest will be a continuation of the analysis with minimum regularity of the eigenfunctions.

REFERENCES

[1] D. Adak, F. Lepe, and G. Rivera, *Vem approximation for the stokes eigenvalue problem: a priori and a posteriori error analysis*, 2022, https://arxiv.org/abs/2212.01961.

[2] D. Adak, D. Mora, and I. Velásquez, *A C^0-nonconforming virtual element methods for the vibration and buckling problems of thin plates*, Comput. Methods Appl. Mech. Engrg., 403 (2023), pp. Paper No. 115763, 24, https://doi.org/10.1016/j.cma.2022.115763.

[3] D. Adak, D. Mora, and I. Velásquez, *Nonconforming virtual element discretization for the transmission eigenvalue problem*, Comput. Math. Appl., 152 (2023), pp. 250–267, https://doi.org/10.1016/j.camwa.2023.10.032.

[4] D. Adak, D. Mora, and I. Velásquez, *Nonconforming virtual element discretization for the transmission eigenvalue problem*, Computers & Mathematics with Applications, 152 (2023), pp. 250–267.

[5] P. F. Antonietti, L. Beirão da Veiga, and G. Manzini, eds., *The virtual element method and its applications*, vol. 31 of SEMA SIMAI Springer Series, Springer, Cham, [2022] ©2022, https://doi.org/10.1007/978-3-030-95319-5.

[6] P. F. Antonietti, G. Manzini, and M. Verani, *The fully nonconforming virtual element method for biharmonic problems*, Math. Models Methods Appl. Sci., 28 (2018), pp. 387–407, https://doi.org/10.1142/S0218202518500100.

[7] M. G. Armentano and V. Moreno, *A posteriori error estimates of stabilized low-order mixed finite elements for the Stokes eigenvalue problem*, J. Comput. Appl. Math., 269 (2014), pp. 132–149, https://doi.org/10.1016/j.cam.2014.03.027.

[8] E. Artioli and L. Mascotto, *Enrichment of the nonconforming virtual element method with singular functions*, Comput. Methods Appl. Mech. Engrg., 385 (2021), pp. Paper No. 114024, 41, https://doi.org/10.1016/j.cma.2021.114024.

[9] B. Ayuso de Dios, K. Lipnikov, and G. Manzini, *The nonconforming virtual element method*, ESAIM Math. Model. Numer. Anal., 50 (2016), pp. 879–904, https://doi.org/10.1051/m2an/2015090.

[10] I. Babuška and J. Osborn, *Handbook of numerical analysis. Vol. II*, (1991), pp. x+928. Finite element methods. Part 1.

[11] L. Beirão da Veiga, F. Brezzi, A. Cangiani, G. Manzini, L. D. Marini, and A. Russo, *Basic principles of virtual element methods*, Math. Models Methods Appl. Sci., 23 (2013), pp. 199–214, https://doi.org/10.1142/S0218202512500492.

[12] L. Beirão da Veiga, F. Brezzi, L. D. Marini, and A. Russo, *Mixed virtual element methods for general second order elliptic problems on polygonal meshes*, ESAIM Math. Model. Numer. Anal., 50 (2016), pp. 727–747, https://doi.org/10.1051/m2an/2015067.

[13] L. Beirão da Veiga, C. Lovadina, and G. Vacca, *Divergence free virtual elements for the Stokes problem on polygonal meshes*, ESAIM Math. Model. Numer. Anal., 51 (2017), pp. 509–535, https://doi.org/10.1051/m2an/2016032.

[14] A. Cangiani, V. Gyrya, and G. Manzini, *The nonconforming virtual element method for the Stokes equations*, SIAM J. Numer. Anal., 54 (2016), pp. 3411–3435, https://doi.org/10.1137/15M1049531.

[15] F. Gardini, G. Manzini, and G. Vacca, *The nonconforming virtual element method for eigenvalue problems*, ESAIM Math. Model. Numer. Anal., 53 (2019), pp. 749–774, https://doi.org/10.1051/m2an/2018074.

[16] J. Gedicke and A. Khan, *Arnold-Winther mixed finite elements for Stokes eigenvalue problems*, SIAM J. Sci. Comput., 40 (2018), pp. A3449–A3469, https://doi.org/10.1137/17M1162032.

[17] J. Gedicke and A. Khan, *Divergence-conforming discontinuous Galerkin finite elements for Stokes eigenvalue problems*, Numer. Math., 144 (2020), pp. 585–614, https://doi.org/10.1007/s00211-019-01095-x.

[18] V. Girault and P.-A. Raviart, *Finite element methods for Navier-Stokes equations*, vol. 5 of Springer Series in Computational Mathematics, Springer-Verlag, Berlin, 1986, https://doi.org/10.1007/978-3-642-61623-5. Theory and algorithms.

[19] P. Huang and Q. Zhang, *A posteriori error estimates for the Stoke eigenvalue problem based on a recovery type estimator*, Bull. Math. Soc. Sci. Math. Roumanie (N.S.), 62(110) (2019), pp. 295–304.

[20] V. John, *Finite element methods for incompressible flow problems*, vol. 51 of Springer Series in Computational Mathematics, Springer, Cham, 2016, https://doi.org/10.1007/978-3-319-45750-5.

[21] T. Kato, *Perturbation theory for linear operators*, Die Grundlehren der mathematischen Wissenschaften, Band 132, Springer-Verlag New York, Inc., New York, 1966.

[22] F. Lepe and D. Mora, *Symmetric and nonsymmetric discontinuous Galerkin methods for a pseudostress formulation of the Stokes spectral problem*, SIAM J. Sci. Comput., 42 (2020), pp. A698–A722, https://doi.org/10.1137/19M1259535.

[23] F. Lepe, D. Mora, G. Rivera, and I. Velásquez, *A virtual element method for the Steklov eigenvalue problem allowing small edges*, J. Sci. Comput., 88 (2021), pp. Paper No. 44, 21, https://doi.org/10.1007/s10915-021-01555-3.

[24] F. Lepe and G. Rivera, *A priori error analysis for a mixed VEM discretization of the spectral problem for the Laplacian operator*, Calcolo, 58 (2021), pp. Paper No. 20, 30, https://doi.org/10.1007/s10092-021-00412-x.

[25] F. Lepe and G. Rivera, *A virtual element approximation for the pseudostress formulation of the Stokes eigenvalue problem*, Comput. Methods Appl. Mech. Engrg., 379 (2021), pp. Paper No. 113753, 21, https://doi.org/10.1016/j.cma.2021.113753.

[26] F. Lepe, G. Rivera, and J. Vellojin, *Mixed methods for the velocity-pressure-pseudostress formulation of the Stokes eigenvalue problem*, SIAM Journal on Scientific Computing, 44 (2022), pp. A1358–A1380, https://doi.org/10.1137/21M1402959.

[27] F. Lepe, G. Rivera, and J. Vellojin, *Finite element analysis of the Oseen eigenvalue problem*, 2023, https://arxiv.org/abs/2311.05321.

[28] H. Liu, W. Gong, S. Wang, and N. Yan, *Superconvergence and a posteriori error estimates for the Stokes eigenvalue problems*, BIT, 53 (2013), pp. 665–687, https://doi.org/10.1007/s10543-013-0422-8.

[29] X. Liu, J. Li, and Z. Chen, *A nonconforming virtual element method for the Stokes problem on general meshes*, Comput. Methods Appl. Mech. Engrg., 320 (2017), pp. 694–711, https://doi.org/10.1016/j.cma.2017.03.027.

[30] C. Lovadina, M. Lyly, and R. Stenberg, *A posteriori estimates for the Stokes eigenvalue problem*, Numer. Methods Partial Differential Equations, 25 (2009), pp. 244–257, https://doi.org/10.1002/num.20342.

[31] D. Mora, G. Rivera, and R. Rodríguez, *A virtual element method for the Steklov eigenvalue problem*, Math. Models Methods Appl. Sci., 25 (2015), pp. 1421–1445, https://doi.org/10.1142/S0218202515500372.

[32] G. Savaré, *Regularity results for elliptic equations in Lipschitz domains*, J. Funct. Anal., 152 (1998), pp. 176–201, https://doi.org/10.1006/jfan.1997.3158.

[33] B. Zhang, J. Zhao, and M. Li, *The divergence-free nonconforming virtual element method for the Navier–Stokes problem*, Numerical Methods for Partial Differential Equations, 39 (2023), pp. 1977–1995.

[34] J. Zhao, S. Chen, and B. Zhang, *The nonconforming virtual element method for plate bending problems*, Math. Models Methods Appl. Sci., 26 (2016), pp. 1671–1687, https://doi.org/10.1142/S021820251650041X.

[35] J. Zhao, B. Zhang, S. Mao, and S. Chen, *The divergence-free nonconforming virtual element for the Stokes problem*, SIAM J. Numer. Anal., 57 (2019), pp. 2730–2759, https://doi.org/10.1137/18M1200762.

[36] J. Zhao, B. Zhang, S. Mao, and S. Chen, *The divergence-free nonconforming virtual element for the stokes problem*, SIAM Journal on Numerical Analysis, 57 (2019), pp. 2730–2759.